universität wien

DISSERTATION / DOCTORAL THESIS

Titel der Dissertation /Title of the Doctoral Thesis

“Gating determinants of CaV1.2 L-type calcium channel”

verfasst von / submitted by

Stanislav Andranovitš

angestrebter akademischer Grad / in partial fulfilment of the requirements for the degree of

Doktor der Naturwissenschaften (Dr. rer.nat.)

Wien, 2019 / Vienna 2019

Studienkennzahl lt. Studienblatt / degree programme code as it appears on the student record sheet:	A 796 610 449
Dissertationsgebiet lt. Studienblatt / field of study as it appears on the student record sheet:	Pharmazie, DK: Molecular Drug Targets
Betreut von / Supervisor:	Univ.-Prof. Dr. Steffen Hering
Mitbetreut von / Co-Supervisor:	

Table of contents

2 APPROBATION OF WORK 5

3 ABBREVIATIONS 7

4 ABSTRACT 9

5 ZUSAMMENFASSUNG 10

6 INTRODUCTION 12

6.1 Voltage gated calcium channels 12

6.2 Subunit composition of high voltage activated calcium channels 14

6.2.1 α_1-subunit 14

6.2.2 β-subunit 16

6.2.3 α_2-δ-subunit 18

6.2.4 γ-subunit 20

7 CLASSIFICATION OF VOLTAGE-GATED CALCIUM CHANNELS 21

8 THE L-TYPE CALCIUM CHANNELS 25

9 ROLE OF CAV CHANNELS IN CARDIAC ACTION POTENTIAL .. 27

10 REGULATION BY CALCIUM CHANNEL BLOCKERS (CCBS) 29

11 CALCIUM CHANNEL GATING 31

11.1 Voltage Dependent Activation 32

11.2 Voltage Dependent Inactivation 33

12 AIM OF THE STUDY 38

13 MATERIALS AND METHODS 39

13.1 Mutagenesis 39

13.2 Cell culture and transient transfection 39

13.3 Ionic current recordings and data acquisition 39

13.4 Analysis of current kinetics 40

14 RESULTS 42

14.1 Principal role of IS4 in activation 43

14.2 IS4 and IIIS4 stabilize the open channel pore 49

14.3 Gradual neutralisation of IS4 charges enhanced voltage-dependent inactivation of CaV1.2 channel 50

14.4 Neutralisation of IIS4 and IIIS4 charges has less effect on voltage dependence of inactivation 55

14.5 Positional specific effects of IVS4 charge neutralisation on voltage dependence of inactivation 57

15 DISCUSSION 58

15.1 Activation is mainly determined by IS4 and to a lesser extent by S4 segments of other domains 58

15.2 Key role of IS4 in CaV1.2 inactivation 60

15.3 Can charge neutralisation in IS4 enhance voltage dependence of inactivation? 61

15.4 Role of IVS4 in inactivation gating 64

15.5 Activation and inactivation of CaV1.2 are linked via segment IS4 64

16 SUMMARY 66

17 ACKNOWLEDGEMENTS 68

18 REFERENCES 69

1 Approbation of work

Publications

1. Hering S, Zangerl-Plessl EM, Beyl S, Hohaus A, **Andranovits S**, Timin EN.

Calcium channel gating.

Pflugers Arch. 2018 Sep; 470(9):1291-1309.

2. **Andranovits S**, Beyl S, Hohaus A, Zangerl-Plessl EM, Timin E, Hering S.

Key role of segment IS4 in CaV1.2 inactivation: link between activation and inactivation.

Pflugers Arch. 2017 Nov;469(11):1485-1493.

3. Saxena P, Hortigon-Vinagre MP, Beyl S, Baburin I, **Andranovits S**, Iqbal SM, Costa A, IJzerman AP, Kügler P, Timin E, Smith GL, Hering S.

Correlation between human ether-a-go-go-related gene channel inhibition and action potential prolongation.

Br J Pharmacol. 2017 Sep;174(18):3081-3093.

4. Beyl S, Hohaus A, **Andranovits S**, Timin E, Hering S.

Upward movement of IS4 and IIIS4 is a rate-limiting stage in CaV1.2 activation.

Pflugers Arch. 2016 Nov;468(11-12):1895-1907.

Public presentations

1. 60th Annual Meeting Biophysical Society,

Los Angeles, United States, March 2016

Poster: "Segments IS4 and IIIS4 contribute most of the effective charge for CaV1.2 activation"

2. 22nd APHAR Symposium: Joint Meeting of the Austrian Pharmacological Society and the Hungarian Society of Experimental and Clinical Pharmacology

Vienna, September 2016

Platform presentation: "Neutralization of the voltage vensor in domain I strongly affects activation and inactivation gating in CaV1.2"

3. The Calcium Channel Network,

Hoi An, Vietnam, October 2016

Platform presentation: "Domain-specific effects of CaV 1.2 voltage sensors on inactivation"

4. MolTag Science Day,

Vienna, November 2016

Poster: “Domain-specific effects of CaV 1.2 voltage sensors on inactivation"

5. Advances in Drug Discovery, Prague Summer School,

Prague, Czech Republic, September 2017

Poster: "Key role of segment IS4 in CaV1.2 inactivation: link between activation and inactivation"

6. 3rd European Calcium Channel Conference

Alpbach, Austria, May 2018

Poster: "Voltage sensors have individual impacts on voltage dependent inactivation"

2 Abbreviations

Å	Angström
CaV	Voltage-gated calcium channel
CCBs	Calcium channel blockers
CDI	Calcium-dependent inactivation
CTC	Charge Transfer Centre
HEK	Human embryonic kidney
HP	Holding potential
HVA	High-voltage-activated channels
I	Current
IC50	Concentration of blocker for 50% inhibition
I-V curve	Current-voltage curve
K_V	Voltage-gated potassium channel
PAA	Phenylalkylamine
qDev	Quaternary devapamil
r300	Inactivation during a 300-ms pulse
τ_{act}	Time constant of current activation
τ_{deact}	Time constant of current deactivation
τ_{inact}	Time constant of current inactivation
$V_{0.5act}$	Voltage of half-maximal current activation
$V_{0.5inact}$	Voltage of half-maximal current inactivation

V_{pulse}	Pulse potential
V_{rev}	Reversal potential
VDI	Voltage-dependent inactivation

3 ABSTRACT

Naturally occurring mutations (causing “channelopathies” [7-9] or mutations introduced to establish structure-activity relationships in CaV may influence gating properties [1-3]. It is generally believed that the voltage-dependent upward movement of VS triggers the opening of CaV1.2 pore while repolarization and the downward movement initiates the channel’s closure [4]. In our study we investigated the individual roles of VSs in the CaV1.2 channel gating.

In order to elucidate the input of individual VSs in CaV1.2 gating, charged residues of segments IS4- IVS4 were replaced by glutamine and the corresponding effects on gating processes (activation, deactivation and inactivation) of calcium channels were analysed [4]. Since, inactivation of L-type calcium channel (CaV1.2) determines the length of the cardiac action potential, our studies mainly focused on this gating process.

During my doctoral thesis work I also contributed to the clarification of the role of individual S4 segments in activation gating [4]. We identified a key role of segment IS4 and IIIS4 in activation. Almost all replacements of charges in IS4 and IIIS4 decreased the slope of the Boltzmann curve of channel activation (activation curve) suggesting a key role of these voltage sensors in channel activation.

The main focus of my project was, however, on the role of S4 segments in inactivation gating. I discovered, that segment IS4 affects not only activation but additionally has a key role in CaV1.2 inactivation. Impairing IS4 function by charge neutralization had by far the largest and regular (charge dependent) effects on voltage-dependent inactivation compared to no or less impact of equivalent charge neutralizations in segments IIS4 and IIIS4 [5].

Interestingly, shifts in the voltage-dependence of inactivation curves induced by IS4 neutralisations showed significant correlation with shifts of the voltage dependence of channel activation. This finding indicates that IS4 movement is not only rate limiting for activation but also initiates inactivation [6].

4 ZUSAMMENFASSUNG

Natürlich vorkommende Mutationen (die zu „Channelopathies“ führen [7-9]) oder zielgerichtet eingeführte Mutationen, um Struktur-Aktivitäts-Zusammenhänge in CaV aufzuklären, können die Gating-Eigenschaften beeinflussen [1-3]. Es wird angenommen, dass die spannungsabhängige Aufwärtsbewegung von Spannungssensoren (VS) die Öffnung der CaV1.2-Pore auslöst, während die Repolarisation die Abwärtsbewegung und das Schließen der Kanäle auslösen [4]. In unserer Studie untersuchten wir die individuellen Rollen von VSs im CaV1.2-Kanal-Gating.

Um die Rolle einzelner VS im CaV1.2-Gating aufzuklären, wurden geladene Aminosäuren der Segmente IS4-IVS4 durch Glutamin ersetzt und die entsprechenden Auswirkungen auf die Gating-Prozesse (Aktivierung, Deaktivierung und Inaktivierung) der Calciumkanäle analysiert [4]. Da die Inaktivierung des L-Typ-Calciumkanals (CaV1.2) die Länge des Herzaktionspotenzials bestimmt, konzentrierten sich unsere Studien hauptsächlich auf diesen Gating-Prozess.

Während meiner Doktorarbeit war ich an Aufklärung der Rolle einzelner S4 -Segmente für die Aktivierung beteiligt [4]. Wir konnten eine Schlüsselrolle von Segment IS4 und IIIS4 bei der CaV1.2-Aktivierung nachweisen. Nahezu alle Ladungsneutralisationen von IS4 und IIIS4 verringerten die Steilheit der Boltzmann-Kurve der Kanalaktivierung (Aktivierungskurve), was auf eine Schlüsselrolle dieser Spannungssensoren für diesen Prozess hindeutet.

Der Schwerpunkt meines Projekts lag jedoch auf der Aufklärung des Einflusses von S4-Segmenten auf die Kanalinaktivierung. Wir fanden heraus, dass das Segment IS4 nicht nur die Aktivierung beeinflusst, sondern auch eine wichtige Rolle bei der CaV1.2-Inaktivierung spielt. Während die Ladungsneutralisierung in IS4 bei weitem die größten und ladungsabhängigen Auswirkungen hatte, führten äquivalente Ladungsneutralisierungen in den Segmenten IIS4 und IIIS4 zu geringeren Effekten auf die spannungsabhängige Inaktivierung [5].

Interessanterweise zeigten Verschiebungen in der Spannungsabhängigkeit von Inaktivierungskurven, die durch IS4-Neutralisierungen induziert wurden, eine signifikante Korrelation mit Verschiebungen der Spannungsabhängigkeit der

Kanalaktivierung. Diese Ergebnisse weisen darauf hin, dass die Bewegung von IS4 nicht nur die Aktivierung beeinflusst, sondern auch die Inaktivierung auslöst [6].

5 Introduction

5.1 Voltage gated calcium channels

Ion channels may be classified by the factors that induce the channel gating. Voltage-gated ion channels opening happens due to the changes in membrane potential. Those that open by the binding of a specific molecule such as a neurotransmitter, hormone or cyclic-nucleotide are called ligand-gated channels [43].

Hodgkin and Huxley first described in detail voltage-gated kinetics of channels selective for Na^+ and K^+ in 1952 [240]. Most of voltage gated channels have different ion selectivity, meaning that they are accessible only to the ions of a certain size and/or charge.

Voltage gated calcium channels are macromolecular structures that span across the cell membrane and allow calcium ions to pass from one side of the lipophilic membrane to the other. These channels were discovered in 1975 by Hagiwara et al. [119]. They are required for many physiological processes in the body like electrical signaling in nerve, muscle contraction, hearing, vision, gene expression and other cellular functions [10, 233, 234].

Conformational changes in the protein structure of these channels leads to their opening making the aqueous pore of the channel accessible to the ions [11, 46] .

The flux of ions through the channels is caused by the difference in the electrochemical gradient between the interior and the exterior of a biological cell. Free intracellular Ca^{2+} is maintained at 10–100 nM in the cytoplasm, a low level relative to the extracellular milieu in the millimolar range.

Ten members of the mammalian CaV channel family have been identified [14].

Calcium channels can thus be subdivided into high-voltage activated (HVA) CaV1.1–1.4, CaV2.1–2.3 and low-voltage activated (LVA) CaV3.1–3.3 channels [15-21],

All CaV channels have a distinct role in cellular signal transduction.

For example, the L-type channels are responsible for contraction, regulation of gene expression, secretion etc. in specialized sensory cells (see Figure1) The CaV2

subfamily is important for synaptic transmission at fast synapses. And T-type channels initiate repetitive firing of action potentials in rhythmically firing cells such as cardiomyocytes [14].

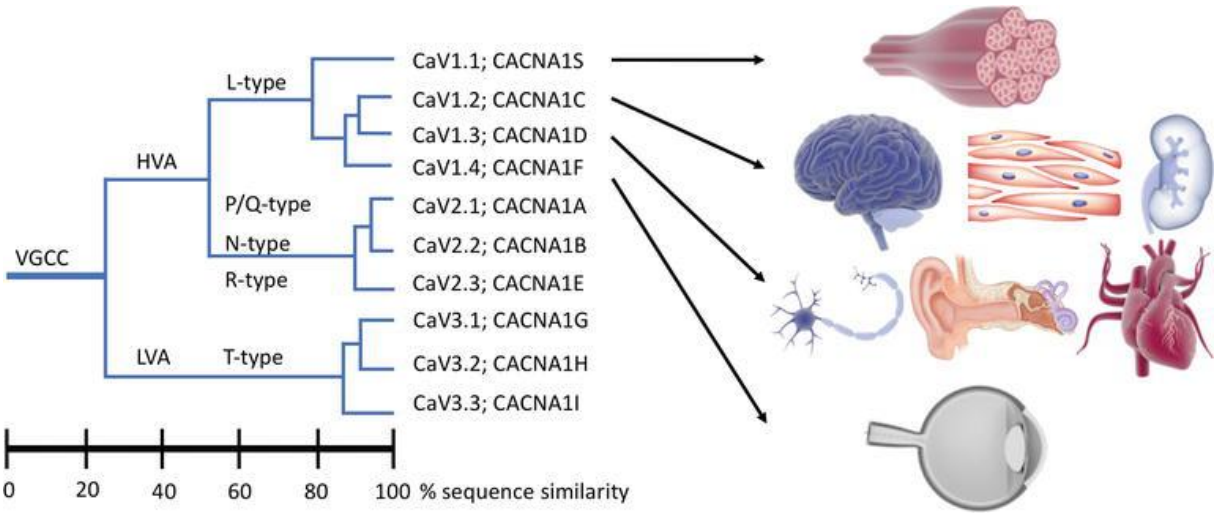


Figure 1.

Evolutionary tree of voltage-gated Ca^{2+} channels [22, 23] and the major distribution of the four L-type isoforms in human tissues [24-26]. The scale in the figure shows the percentage of sequence identity in the α1 subunit of different channels. (Figure from Feng et. al [27]).

Moreover CaV are involved in various pathological processes that occur in neuronal, neurosecretory, muscle and other cells [28]. Mutations of CaV can cause abnormalities in channel functioning resulting in diseases such as ataxia, migraine, epilepsy [29], [30], night blindness, intellectual impairment [7]. CaV1.2 play important role in neuropsychiatric disease and mutation in these channel cause Timothy syndrome [9]. CaV1.1 are in involved in hypokalemic periodic paralysis and malignant hyperthermia [31] . CaV1.3 channel activity may contribute to Parkinson disease pathology by multiple mechanisms [32, 33], as well as the channels may be involved in hearing [34] and cardiac dysfunction [35], neuropsychiatric disease [36]. Mutations in CaV1.4 can cause Congenital Stationary Night Blindness of Type 2 [37].

Recently, Wu et al. published full-length cryo-EM structures of CaV1.1 (rabbit) α1 subunits composed of an α1S, an extracellular α2δ, an intracellular β, and γ subunit first with an overall resolution of 3.6 and later of 4.2 Å [38, 39]. The reported structural data revealed a high degree of structural homology of pore forming subunit of CaV1.1 to other voltage-gated ion channels [4].

The sequence identity between the two L-type channels: CaV1.1 and CaV1.2 channels is high (55% in human channels). Especially, the region of voltage-sensitive segments and its charged residues are highly conserved [6]. Therefore, the provided by Wu et al. crystal structure provides new opportunities for the modeling.

5.2 Subunit composition of high voltage activated calcium channels

Voltage-gated calcium channels are composed of several subunits: the pore forming α_1-subunit and the auxiliary $\alpha_2\delta$, β and γ subunits [40, 41] .

The auxiliary subunits $\alpha_2\delta$, β and γ are encoded by 4, 4 and 8 different genes respectively. The subunit composition of a calcium channels may have dramatic effects on their functional and pharmacological properties [42].

5.2.1 α_1-subunit

The α1 subunit is the transmembrane subunit forming the voltage-sensitive, calcium-selective pore [41]. α –subunits are 1800–2300 amino acids long and have molecular weight of around 190–250 kDa [43].

The α1 subunit is composed of four concatenated domains (I - IV), and each domain bears six transmembrane segments (Figure2B). These domains share a common architecture with other members of the voltage-gated ion channel superfamily [44].

The first four segments of each domain (segments S1–S4) form the voltage-sensing domain, while the remaining two (S5 and S6) form the calcium-selective pore [45].

The S4 transmembrane segments of CaV channels contain positively charged amino acids (arginines or lysines), which are located in every third or fourth position of the alpha helix [11, 46]. The sequence and number of amino acids is unique for every single VS in CaV channels.

For the outward movement of the VS the „sliding-helix model" was proposed [46] where the influence of an electric field, each VS moves outward and rotates during activation thereby initiating the conformational change allowing the pore channel to open. However, the precise molecular mechanism underlying voltage sensing in CaV remains elusive [47].

It was previously shown that potassium and sodium voltage-gated channels have so called ‘‘gating charge transfer center’’ (CTC) [48-50]. Corresponding to CTC residues are also conserved in CaV channels [47].

This center includes highly conserved residues: a phenylalanine in S2 and negatively charged residues in S2 and S3.

In the latest CaV1.1 structure [38] , the electron density map quality of the VSDIII does not allow assignment of the residues on S3 and S4. The authors propose the VSs are in a depolarized or upstate. In VSDI, four charges, R1 to R4, are above the occluding hydrophobic residue, in this case a phenylalanine, of the CTC. In VSDII, only three charges, R2 to R4, are above the occluding phenylalanine, suggesting individual and asynchronous movements of S4 segments [5].

DeCaen et al. [51] have shown in disulfide locking experiments on modified bacterial sodium channel (NaChBac), that the gating charges in S4 segments sequentially form ion pairs with negatively charged and polar residues located in the neighboring S1, S2, S3-segments [52].

The outward movement of VS through a hydrophobic environment without any facilitation would be energetically prohibitive [46]. The interactions between S4 and neighboring transmembrane segments catalyze and stabilize the movement of VS through the dielectric interior of the plasma membrane [47]. The charges of S4 build transient hydrogen bonds (H-bonds) with the negative charges of S2 and S3 as VS sequentially passes through the CTC [47, 50, 53-55].

The pore region of CaV contains the putative selectivity filter, that ensures high selectivity of the channel pore for calcium ions. It is located at the extracellular side of the transmembrane domain (TMD) and contains negatively charged residues. In HVA channels the filter contains four glutamates (the EEEE locus) and in T-type channels two glutamate and two aspartate residues (EEDD locus) [5, 38, 39, 56-58].

The selectivity filter extends to the channel CaVity, which is surrounded by a tetrameric arrangement of the S5 and S6 helices (see Figure 7) [5]. The S6 helices form the

activation gate at the intracellular end of the transmembrane domain [241]. In the closed state, the pore-lining S6 helices converge at the intracellular side to obstruct ion permeation [5]. S5 and S6 segments contain interaction sites for various activators and blockers [5, 59, 60].

The cytosolic part of α1-protein comprises N and C-termini and the interdomain regions (called the I-II, II-III and III-IV loops) [45]. These domains are important for the channel regulation and represent binding sites for several signalling molecules. Several studies have shown that N- and C-termini interaction play an important role in the inactivation of the channel, and in gating in general [61]. The I – II loop contains a binding site for the beta subunits [62].

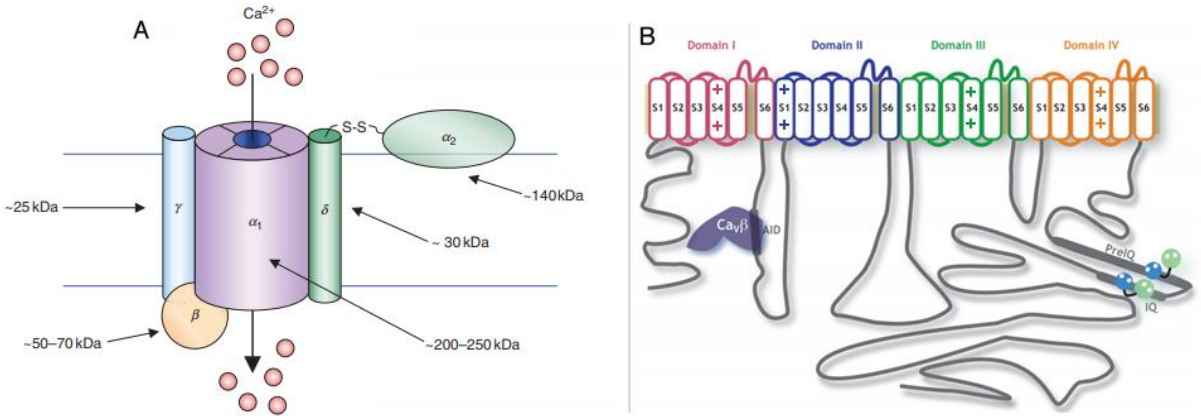


Figure 2.

(A) Schematic diagram of the high-voltage activated L-type calcium channel. The complex consists of pore forming α_1-subunit and the auxiliary $\alpha_2\delta$, β and γ subunits. (Figure modified from Snutch [63])

(B) Topology of the α1 pore-forming subunit. Four domains are shown each containing six transmembrane segments S1-S6. The fourth transmembrane segment (S4) in each domain bears positive charges. β-subunit (shown in purple) has an interaction site (called "AID") on the I-II intracellular loop. Calmodulin (CaM) binds to the IQ domain of C-terminal cytoplasmic tail. (Figure modified from Minor et al. [62]).

5.2.2 β-subunit

Association between auxiliary β and α_1-subunits is obligatory for forming functional high-voltage-activated Ca^{2+} channels (See Figure2) [64] .β-subunits are required for

efficient membrane trafficking of pore-forming subunit to the cell membrane [65-68], increase channel open probability [69], affect channel gating properties [70-73] and drug sensitivity [42], protect the channels from endoplasmic reticulum-associated proteasomal degradation [74, 75]. *β* as well as *α2δ* subunits play important roles in channel folding [76].

The importance of β-subunits for normal body functioning is demonstrated in knockout mice models. For instance, β_1 knockout causes asphyxiation [77] and β_{2a} knockout embryonic lethal due to cardiac defects [78].

There are four mammalian isoforms, encoded by CACNB1, CACNB2, CACNB3, CACNB4 genes. Interestingly, each isoform has separate effects on voltage-dependent inactivation: CaVβ1b and CaVβ3 speed inactivation and CaVβ4 causes moderate slowing [79].

The first β-subunit (CACNB1) was identified in the purified skeletal muscle DHP receptor calcium channel complex [80], three other β-subunit genes were cloned by homology with CACNB1 [71, 81, 82].

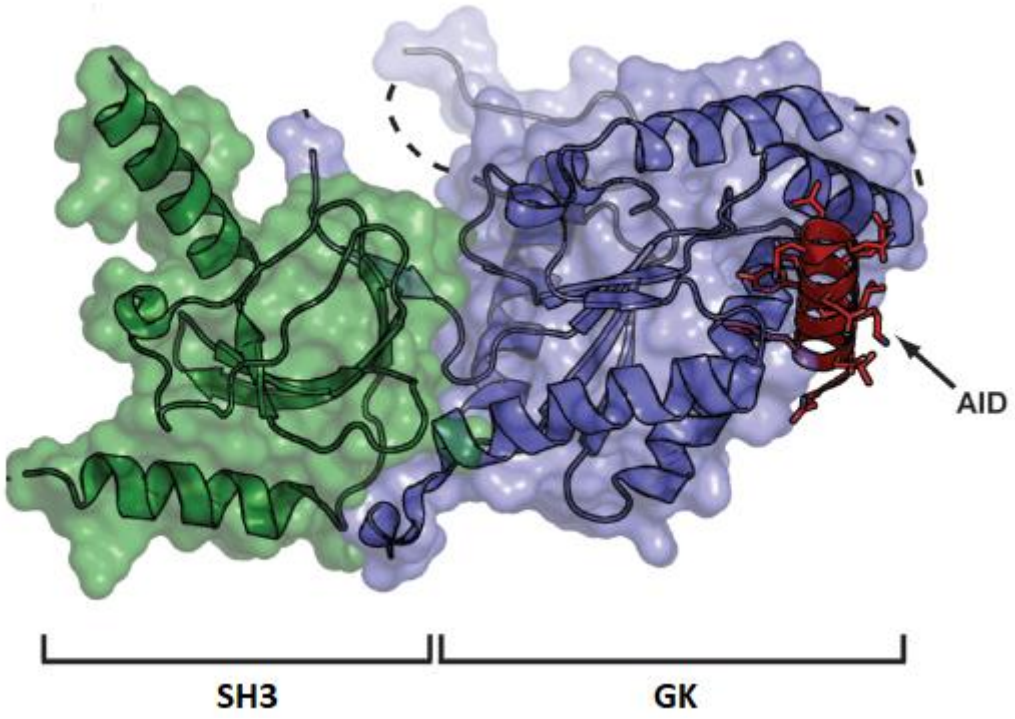


Figure 3.

Interactions between β-subunit and I-II linker . (A) Structure of the β-AID complex. SH3 domain is shown in green and GK in blue. α-interaction domain (AID) is shown in red with the sidechains (sticks) (Figure modified from Minor et al. [62]).

A modelling study showed that β-subunit contains a guanylate kinase (GK) domain and an SH3 (src homology 3) domain [83, 84].

The association between the *α*1 and *β* subunits is quite robust, the GK binds to the α-interaction domain (AID) which is in the proximal part of the I-II linker [45, 62, 76] (See Figure3).

5.2.3 α_2-δ-subunit

The α2δ-subunit plays an important role in calcium channel folding and their trafficking to the cell surface [85]. This subunit represents a target of gabapentinoid drugs (gabapentin (Neurontin) and pregabalin (Lyrica)), making it particularly important for pharmacology [86, 87].

At the moment four types of α2δ proteins are known (*α2δ*-1, *α2δ*-2, *α2δ*-3, *α2δ*-4) and they have generally a similar structure ([88],[89],[85]). A single gene encodes the α2δ protein, that is posttranslationally cleaved into α2 and δ subunits [90]. α2 and δ are disulfide-bonded together ([91],[90]) and have combined molecular weight of 170 kDA. The cysteines residues involved in this bond were determined for *α2δ*-1 [92].

The α2 represents an extracellular part of α2δ subunit and interacts with the pore-forming subunit of the channel. All *α2δ*-subunits contain a Von Willebrand factor-A (VWA) domain within the α2 moiety [93] that contains a metal ion binding site, and docks to three different extracellular loops on the CaVα1 subunit [21, 76].

A key motif in VWA domains is the metal ion-dependent adhesion site (MIDAS) that confers divalent metal (usually Mg^{2+})-dependent binding to the ligand [94]. Mutation of the MIDAS motif reduces the trafficking of the α1 subunit to the cell membrane [93]. Therefore, the perfect MIDAS motif is required for increasing calcium currents [93, 95]. In case of α2δ-1 and α2δ-2 the MIDAS motif has full complement of five polar residues [93], whereas α2δ-3 and α2δ-4 have one residue missing [76].

The role of δ segment is the anchoring of α2δ subunit to the extracellular leaf of the plasma membrane via glycophosphatidyl moiety attached to a cysteine residue [86].

The α2δ subunits influence the channel's biophysical properties, including voltage dependence and inactivation kinetics; in particular they consistently increase the inactivation rate, although to different extents [76]. The greatest effect was observed for *α2δ*-1 [76].

α2 domain may provide the elements modulating channel activation [96] while *δ* subunit complex appears to be important for the shift of the steady-state inactivation and modulation of the inactivation kinetics [97, 98].

It was found that α2δ-1 subunits in CaV1.2, exerted little effect on the activation voltage dependence [70, 99-102]. However, in other studies a hyperpolarization of activation was reported [97].

It was found for several different calcium channel isoforms that the *α2δ* subunits shifted the steady-state inactivation curve into the hyperpolarizing direction [70, 97, 103, 104]. This shift was confirmed for cardiac calcium channel currents in *α2δ*-1 knockout mice [105].

Generally, the α2δ subunits have been found to increase the calcium channel expression [96, 101, 104]. Combination of CaV2.1 with β4, typical for cerebellar Purkinje cells, resulted in 3-fold increase of calcium current [106, 107] . However, α2δ-2 did not increase the single channel conductance. The changes in the current amplitude is presumably solely due to an increase in the number of functional channels at the cell surface [106].

Recently a high resolution cryo-EM structure of the CaV1.1 calcium channel complex purified from skeletal muscle was published by Wu et al. It has identified multiple interactions of *α2δ*-1 with several extracellular loops in domains I–III of CaV1.1 [39, 108].

5.2.4 γ-subunit

The γ-subunit is a glycoprotein composed of four transmembrane spanning helices and two N-glycosylation sites (Figure4) [109]. It contacts the voltage-sensing segment of the fourth domain (Figure2A) [38]. IVS3 and IVS4 segments of α1c have a number of A large number of hydrophobic residues that interact with residues of TM2 and TM3 of γ-subunit (Figure4) [38].

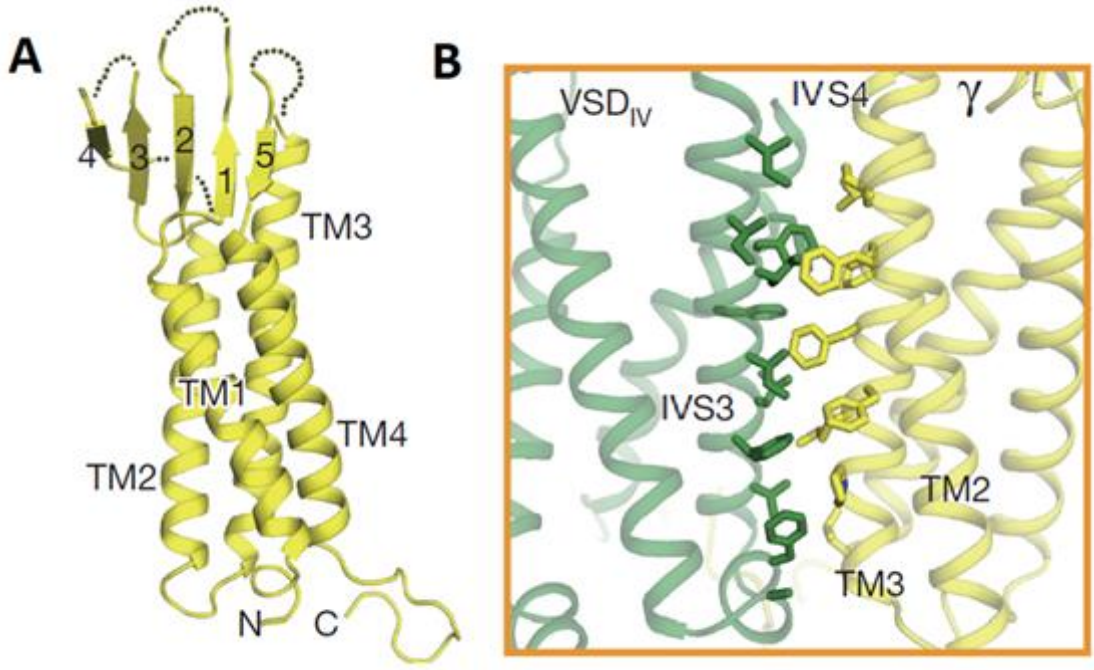


Figure 4.

a, γ–subunit consist of four transmembrane helixes (TM1,TM2,TM3 and TM4). b , The interaction between *α1c* and , γ–subunit is mediated by van der Waals contacts between hydrophobic residues in helices 2 and 3 (TM2 and TM3) in γ and IVS3 and IVS4 (Figure modified from Wu et al. [38]).

There are 8 types of γ-subunits, encoded by CACNG1, CACNG2, CACNG3, CACNG4, CACNG5, CACNG6, CACNG7 and CACNG8 genes [110]. The first γ-1 subunit was identified in muscle by Glossmann et al. [111]. This subunit is associated with skeletal muscle and no expression was observed in heart, liver, kidney, spleen, stomach, or brain [112]. *γ*-1 is involved in the modulation of the inactivation kinetics and current amplitude of the skeletal voltage- gated calcium channel [113]. γ-6 as well as *γ*-1 is associated with L-type skeletal muscle calcium channel complex [113].

γ-2, *γ*-3, *γ*-4, *γ*-5, *γ*-7 and *γ*-8 are mainly expressed in brain and may be expressed in heart and lung tissues as well [113]. No of these subunits have been shown to form an integral part of neuronal [114, 115] or cardiac calcium channels [116]. However, they have well-defined roles as transmembrane AMPA glutamate receptor modifying proteins [117].

The effects of the various γ subunits on voltage-gated calcium channels activity is small [110].

6 Classification of voltage-gated calcium channels

In mammals, CaV channels constitute a family encoded by at least 10 genes [47]. Each α_1-subunit due to alternative splicing has multiple variants and it gives rise to functionally diverse channels. To fulfill their diverse functions CaV channels activate at substantially different membrane potentials ranging from about -55 mV in T-type channels to +50 mV mV in HVA channels [47, 62, 118].

CaV channels mediate a range of cellular functions like: plateau of the cardiac action potential, contraction of muscle cells, generation of pace maker potentials, the release of hormones and neurotransmitters, sensory functions, and gene expression [14, 24, 60, 86].

Historically, several classifications were used for calcium channels. Low-voltage activated (LVA) channels can be activated by small depolarizations of the plasma membrane while high-voltage activated (HVA) channels require relatively larger depolarizations to open [18, 119, 120].

HVA channels, also known as L-type channels (L for large and long-lasting) activate around –20 mV and are characterized by a large single channel conductance (15-25 pS) [235] and slow current activation kinetics, slow voltage-dependent inactivation and specific inhibition by calcium antagonist drugs [14, 121, 122].

HVA channels are also designated L-type, as they have slow voltage dependent inactivation and therefore are long lasting and large current [122] . L-type channels are broadly found in different muscle tissues (smooth, skeletal and cardiac).

Hagiwara et al. first revealed LVA calcium currents in starfish eggs in 1975 [119]. Decade later LVA currents were subsequently characterized in detail in voltage-clamped dorsal root ganglion neurons [14, 16, 123, 124].

LVA calcium channels activate at membrane voltage positive to –70 mV, have small single channel conductance, inactivate rapidly and deactivate slowly. They are also named T-type calcium channels because of their tiny and transient currents.

LVA currents inactivate faster, more completely, and at more negative membrane potentials than HVA currents [18].

Recordings from dissociated dorsal root ganglion neurons revealed an additional calcium current, that was designated N-type (N-neuronal) [124].

N-type currents have single-channel conductance between T- and L-type; more negative and faster rate of inactivation than L-type but more positive and slower than T-type [14, 124]. They are involved in the pain processing, and send pain signals from the peripheral nervous system to Central Nervous System [125].

These channels are insensitive to conventional L-type calcium channel blocker, the first and best characterized blocker of these channels is a toxin component from the marine snail *Conus geographus*, ω-conotoxin [122, 126, 127]. This toxin is highly selective to N-type channels [128, 129] and was used to show that N-type calcium currents play a key role in neurotransmitter release [130].

In 1980 Llinás and Sugimori first recorded in Purkinje neurons new type of current, that was not blocked by DHPs or by ω-conotoxin [120]. This current was called P-type (for Purkinje) and is selectively blocked by ω-agatoxin derived from the spider venom of *Agelenopsis aperta [131]*.

Q-type Ca^{2+} currents were first recorded in cerebellar granule neurons [132] and are also blocked by ω –agatoxin, but with a lower affinity, than P-type [14].
Usually P and Q channels are combined in one group and are called PQ currents [126].

R-type Ca^{2+} channels are resistant to both organic L-type Ca^{2+} currents antagonists and the peptide toxins specific for N-type or P/Q-type currents [133].

Another classification of CaV channels refers to the genes encoding α_1-subunits [14]. Altogether ten α1-subunits have now been cloned. They all have specialized functions and distributions in the body (summarized in Table 1). First, the cloning of the α1s -subunit from skeletal muscle was accomplished [134, 135] .

Later α1-subunits from heart and smooth muscle were cloned and named α1c-a and α1c-b respectively [136, 137]. Then two more L- type calcium channels were identified α1d, cloned from brain [138, 139] . And α1f was identified because of its role in a genetic form of night blindness [140, 141].

Several brain calcium channels, encoding P/Q- and N-type channels, were cloned and dubbed α1a and α1b respectively [142-144]. Another brain calcium channel was cloned and termed α1e [133].

Genes for the three members of the T-type calcium channels were later cloned by Perez-Reyes and colleagues: α1g [145], α1h [145] and α1i [146].

After the cloning and initial characterization of all α1-subunits a rational nomenclature was adopted [23, 147]. All α1 subunits were grouped into CaV1 (L-type), CaV2 (non-L-type) and CaV3 (T-type); see the Table 1.

Table 1. Physiological functions, pharmacology and pathologies associated with calcium channels .

Channel	Current	Localization	Specific Antagonists	Cellular Functions	Inherited Disease
CaV1.1 (α_{1S})	L	Skeletal muscle, transverse tubules	Dihydropyridines, phenylalkylamines, benzodiazepines	Excitation-contraction coupling	Hypokalemic periodic paralysis, malignant hyperthermiasusceptibility

CaV1.2 (α_{1C})	L	Cardiac myocytes (atrial and ventrical),smooth muscle myocytes, endocrine cells, neuronal cell bodies, proximal dendrites,	Dihydropyridines, phenylalkylamines, benzodiazepines	Excitation-contraction coupling, hormone release, regulation of transcription, synaptic integration	Timothy syndrome: Cardiac arrhythmias, developmental abnormalities, and autism spectrum disorders. Brugada syndrome: abnormal electrocardiogram, sudden cardiac death
CaV1.3 (α_{1D})	L	Endocrine cells, neuronal cell bodies, cardiac atrial myocytes and pacemaker cells, cochlear hair cells	Dihydropyridines, phenylalkylamines, benzodiazepines	Hormone release, transcription regulation, synaptic regulation, cardiac pacemaking, hearing, neurotransmitter release from sensory cells	Sino-atrial node dysfunction and deafness
CaV1.4 (α_{1F})	L	Retinal rod and bipolar cells, spinal cord, adrenal gland, mast cells	Dihydropyridines, phenylalkylamines, benzodiazepines	Neurotransmitter release from photoreceptors	Stationary night blindness
CaV2.1 (α_{1A})	P/Q	Nerve terminals and dendrites, neuroendocrine cells	ω-agatoxin IVA	Neurotransmitter release, dendritic Ca^{2+} transients, hormone release	Familial hemiplegic migraine, spinocerebellar and episodic ataxias

CaV2.2 (α_{1B})	N	Nerve terminals and dendrites, neuroendocrine cells	ω -CTx-GVIA	Neurotransmitterrelease, dendritic Ca^{2+} transients, hormone release	
CaV2.3 (α_{1E})	R	Neuronal cell bodies and dendrites	SNX-482	Repetitive firing, dendritic Ca^{2+} transients	
CaV3.1 (α_{1G})	T	Neuronal cell bodies and dendrites, cardiac myocytes	TTA-A2, TTA-P2	Pacemaking, repetitive firing	Idiopathic generalized epilepsy, autism spectrum disorders
CaV3.2 (α_{1H})	T	Neuronal cell bodies and dendrites, cardiac and smooth muscle myocytes, other tissue	TTA-A2, TTA-P2	Absence epilepsy, autism spectrum disorders	
CaV3.3 (α_{1I})	T	Neuronal cell bodies and dendrites	TTA-A2, TTA-P2	Pacemaking, repetitive firing	

Modified from Barker et al., 2017 [43]

7 The L-type calcium channels

L-type Ca^{2+} channels consist of CaV1.1-CaV1.4 subtypes.

Not only long-lasting currents with slow voltage-dependent inactivation distinguishes L-type channels from other Ca^{2+} channels, but also their high sensitivity to DHPs [148]. L-type channels were found in different tissues, like brain, heart, smooth and skeletal muscle. Their localization in these tissues was detected by the use of the radioactive derivatives of the calcium channel blockers (CCBs).

The skeletal muscle L-type channel (CaV1.1) a1 subunit, is encoded by the CACNA1S gene, CaV1.2 by CACNA1C, CaV1.3 a1 subunit by CACNA1D [23] and .CaV1.4 by CACNA1F [140, 141].

Interestingly, in the heart CaV1.2 and CaV1.3 differentially contribute to the various anatomical regions.

CaV1.2 is the most widely expressed L-type calcium channel and is mainly found in cardiomyocytes. The voltage-dependence of activation of CaV1.2 occurs at higher voltages than CaV1.3 but at lower voltages than CaV1.1a [149].

Due to the left shift of activation curve around 9-15 mV (compared to CaV1.2), CaV1.3 channels open at threshold potentials and are generally involved in the pacemaking activity and stabilization of plateau potentials [60]. CaV1.3 predominate in the in the sinoatrial and atrioventricular nodes [150]. Indeed, loss-of-function mutation in CaV1.3, leads to the loss of the normal pacemaking function human in form of bradyarrhythmia [34].

Cardiac disease can result not only from the loss of function of calcium channels but also from their enhanced activity. Increase in calcium influx through CaV1.2 (without major kinetic changes in the current) due to overexpression of auxillary β-subunits induces cardiac hypertrophy in a mice model [151].

CaV1.1 and CaV1.4 are not significantly distributed in the human body and they are expressed mainly in several tissues. CaV1.1 is mainly expressed in skeletal muscle and is involved in muscle contraction. CaV1.4 is essential for normal vision and is found in the retina. The level of expression of these two subtypes in the brain is not significant, but can not be excluded [152].

L-type channels undergo extensive alternative splicing that can affect their gating properties and protein interactions which allows them to serve different physiological functions [60].

8 Role of CaV channels in cardiac action potential

The influx of Ca^{2+} ions through L-type channels is needed for proper cardiac function. In ventricle CaV1.2 is the only CaV channel, whereas both CaV1.2 and CaV1.3 are expressed in atrial part of the heart [136] (See Table 1).

Subtle perturbations in function of these channels lead to profound diseases: mice with global deletion of the gene encoding a1c-subunit have abnormal embryonic cardiac function and morphogenesis [153], and knockout of the CaV1.2 gene in adult mouse heart results in reduced myocardial contractility and lethality [154].

The mutations in genes encoding a1c-subunit of CaV1.2 induce several channelopathies. For instance, the Timothy syndrome is a multi-system disorder with QT-prolongation, heart arrhythmias, structural heart defects, cognitive abnormalities, immune deficiency, hypoglycemia, and syndactyly [155]. The disease is caused by mutations G402S and G406R, that abolish inactivation of CaV1.2 [156]. The subsequent increase in Ca^{2+} entry results in cytotoxicity [1, 157].

A sudden death syndrome results from a loss of function of the α1 or β2b subunit of the L-type Ca^{2+} channel and is characterized by symptoms like ventricular fibrillation or polymorphic ventricular tachycardia [6] .

L-type channels are major contributors to the action potential plateau phase and mediate the shape of the cardiac action potential [158].

The resting membrane potential of ventricular cardiac cells is around -90 mV. At the resting potential main ions found outside the cell are Na^{+}, and Cl^{-}, whereas inside the cell it is mainly K^{+} [159].

The cardiac action potential can be subdivided into five phases (Figure 5) [160]. Phase 0 corresponds to the period of rapid depolarization due to the Na^+ channels opening, that rises membrane potential to positive value around +50 mV. Phase 0 is followed by phase 1 (early repolarization), which is characterized by termination of the depolarizing inward Na+ current and activation of the transient outward K^+ (I_{to} - channels) [159].

The initial influx of sodium ions triggers voltage-gated activation of calcium channels (~ at -30mV for CaV1.2), subsequent release from the sarcoplasmic reticulum (SR) via activation of type 2 ryanodine receptors (RyR2) ,and finally, contraction of the sarcomeres [161].

The CaV1.2 dominates Phase 2 and triggers excitation–contraction coupling (EC). These channels are located within 15nm of SR in a structure called „couplon“ [162]. The influx of calcium ions activates RyR2 (intracellular calcium channels of SR), which produces Ca^{2+} sparks and activates muscle contraction [163]. Interestingly, the opening of single or only small cluster of CaV1.2 is needed for the Ca^{2+} spark activation [164, 165].

Phase 2 represents mainly a balance between the depolarizing L-type Ca^{2+} current and hyperpolarizing K^+ currents [166]. Release of Ca^{2+} from the SR, via calcium-induced calcium release is vital for the plateau phase of the action potential [167].

In Phase 3 Ca^{2+} currents are reduced and several K^+ channels (IKs, IKr, IK1) open. Finally, the membrane potential is repolarized to the initial diastolic membrane potential of quiescent ventricular myocytes (Phase 4) [159].

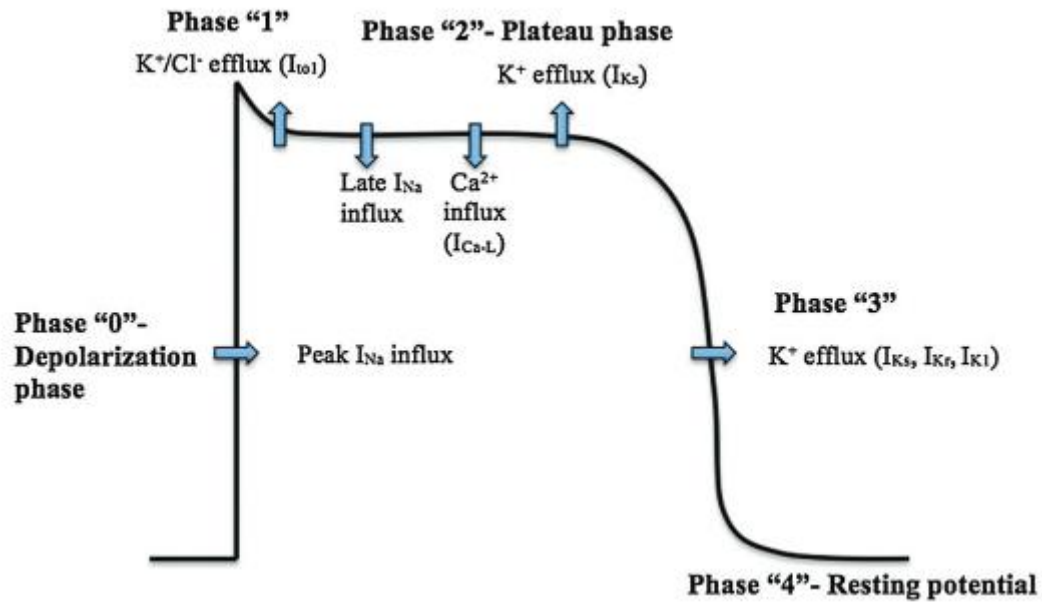


Figure 5.

A typical action potential (AP) waveform of a healthy adult human ventricular myocyte illustrating ionic currents during its different phases (0-4) (Figure from Saad et al.) [168]

9 Regulation by calcium channel blockers (CCBs)

CCBs are generally classified into three major groups according to their chemical structure: dihydropyridines (amlodipine, felodipine, isradipine, nicardipine, bepridil, nifedipine etc.), phenylalkylamines (fendiline, gallopamil, verapamil etc.) and benzothiazepines (diltiazem) [169].

There are several CCBs, that do not belong to any of three main groups. For instance gabapentinoids (gabapentin, pregabalin) [87]. Furthermore, calcium channel inhibition was reported for the class III antiarrhythmic Amiodaron [236] and other non cardiac drugs such as antidepressants and others [237] suggesting that calcium channel inhibition is an accompanying phenomenon for several non-cardiovascular drugs.

Verapamil was the first selective organic „calcium antagonist drug" discovered. It was described in 1960s by a German pharmacologist and physiologist Albrecht Fleckenstein, who defined calcium antagonist as any molecule that would block excitation–contraction coupling in the same way as removal of external Ca^{2+} [22, 170]

CCBs are mainly used to cure different heart diseases (hypertension, ischemia, angina pectoris etc). Pharmacological inhibition of CaV1.2 induces antihypertensive and anti-ischemic effect, predominantly reducing peripheral vascular resistance and negative inotropy [60]. Inhibition of L-type channels in the sinoatrial node (SAN) induces bradycardic effect due to CaV1.3 pacemaker current block and the block of CaV1.2 channels, that support action potentials. Action of CCBs is usually enhanced by membrane depolarisations ([171,172, 173]). It may be explained by a higher affinity of these drugs to open and/or inactivated channels. Consequently, some classes of CCBs (e.g. PAAs, diltiazem) inhibit high voltage activated calcium channels in a “use-dependent” manner.

Despite different structure of dihydropyridines (DHPs), phenylalkylamines (PAAs) and benzothiazepines (BTZs) they all bind to three separate, but allosterically interacting, receptor sites on CaV1.2 channels close to the activation gate and the channel pore [174, 175]. Although the mechanism of the block remains different.

The DHPs are thought to act as allosteric modulators of voltage-dependent Ca^{2+} channel activation, whereas PAAs and BTZs are supposed to physically block the pore [176].

Tang et al. [176] have used crystallographic and functional analysis to study Br-verapamil and amlodipine binding to CaVAb (bacterial homotetrameric CaV channel model). Authors speculate that the binding site for DHPs is located on the external, lipid-facing surface of the pore module, positioned at the interface of domains III and IV. This finding is in the line with previous data received from photoaffinity labelling and antibody mapping studies, where it was shown that all three classes of CCBs bind to the transmembrane region of domain IV of the α_1-subunit [177,178,179] with additional sites on domain III [177, 180]. Furthermore, alanine-scanning mutagenesis has revealed that amino acid residues that affect sensitivity to CCBs are located in the same domains, exactly in segments IIIS5, IIIS6 and IVS6 [181].

DHPs binding allosterically induces an asymmetric conformation of the selectivity filter, inducing Ca^{2+}-mediated block of the pore. Interestingly, that despite the 4-fold symmetry of the channel, only one DHP molecule can be bound at a given time [21].

In contrast, PAAs interact with S6 helices in the central cavity on the intracellular side of the ion selectivity filter and physically block the ion-conducting pathway [176].

Interestingly, in the absence of CCBs interaction sites both for DHPs and PAAs are normally occupied by membrane lipids ,suggesting that this drug interaction site has the normal function of interacting with the plasma membrane [21].

10 Calcium channel gating

CaV channels can stay in different conformations (Figure 6) [5]:

1. Resting-closed **(R)** : pore is closed and VSs lock the pore
2. Activated closed state **(A)**: pore is closed, but the VSs are in their up position
3. Open (**O**) : pore is open and the VSs are in the up position,
4. Deactivated-open (**D**) : pore is still open though the VSs are in their down position [5]

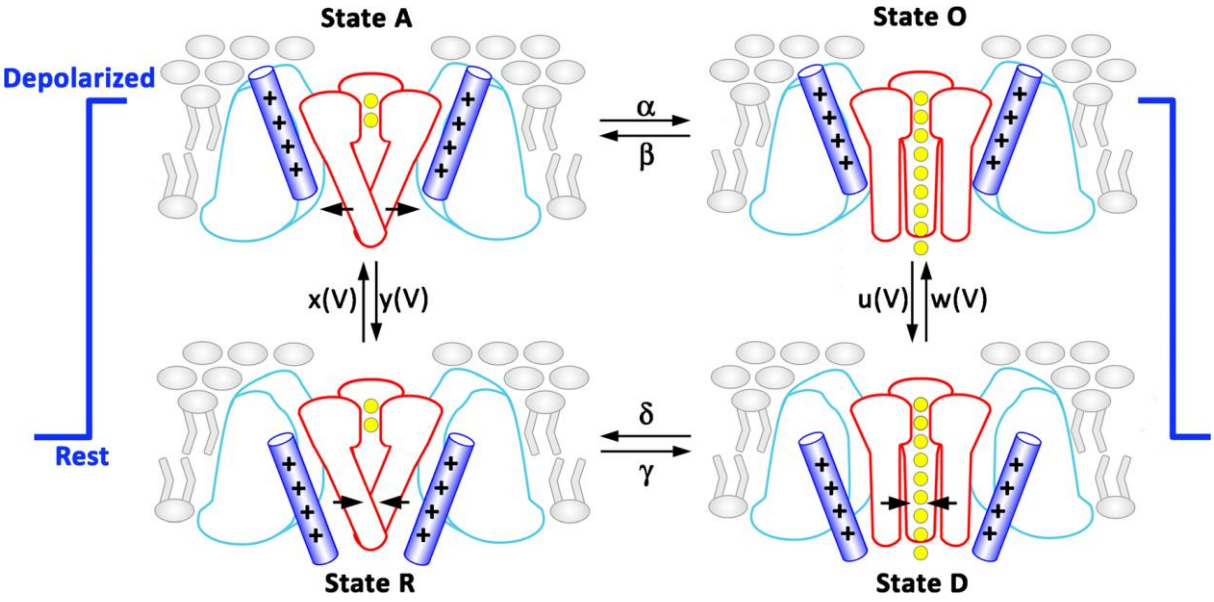


Figure 6.

State transitions during activation (modified from Beyl et al. [182]) Activation gating is determined by two functionally separate processes: a voltage-sensing mechanism (++++) and the conducting pore. Each functional unit can dwell in two states: the VS in the resting (down) and activated (up) states and the pore in the open or closed states. The entire molecule therefore dwells in 2 × 2 = 4 states: R, pore is closed and voltage-sensing mechanism locks the pore; A, voltage-sensing mechanism is activated and releases the pore, which, however, remains closed; O, the pore is open; D, the deactivated voltage-sensing mechanism is in the down position while the pore is still open. Rate constants of the pore opening and closure (α, β, γ, δ) are assumed to be

voltage independent. Rate constants of voltage-sensing mechanism (x, y, u, and w) are voltage dependent. Figure modified from Hering et al. [5].

It is believed that pore opening of CaV is initiated by the voltage-dependent upward movement of positively charged S4 while its downward movement during repolarization forces the channel to close [4].

The determinants of the opening and closing of the CaV pore are at least two sub-processes: movement of VSs and opening and closure of S6 gates [5].

10.1 Voltage Dependent Activation

In 1952 Hodgkin and Huxley were first who hypothesised that charged particles movement across the cell membrane ("gating current") initiates the activation of voltage-gated ion channels [183]. Later this charge movement was directly measured for NaV channels by Armstrong and Bezanilla [184].

According to Zagotta et al. [185]., channel activation involves charge movement in four domains followed by a 'concerted' step of pore opening. Multiple investigations support the view that in this chain of events, the concerted pore opening is a rate-limiting stage [4].

Several groups tried to elucidate the role of VSs in CaV activation. For instance, Yamaguchi et al., suggested that VSs with a proline (IS4 and IIIS4) facilitate opening of CaV1.2 to a greater extent than the ones without a proline (IIS4 and IVS4) [186].

Tuluc et al. [187] performed mutagenesis studies in CaV1.1 channels and pointed to a major role voltage sensor of domain IV the in the–voltage dependence of CaV1.1, whereas VS of domain I seems to be the major determinant of the kinetics of activation [187].

Jurkovicova-Tarabova et al. neutralized the uppermost charge in VSs of CaV3.1 channel, exchanging arginines for cysteins and compared the ratio G_{max}/Q_{max} of several mutant combinations. The main outcome of the work was that the domain I,

like in the study of Beyl et al., plays the main role for the activation of CaV3.1, whereas VSs of domains II and III are less important [188].

Karmažínová et al.[189] proposed that activation of IS4 in CaV3 represents a rate limiting stage in activation suggesting a general role of this segment in CaV channel gating .

In contrast, voltage-clamp fluorometry studies of Pantazis et al. showed that VSs of domain II and III together contribute about 85% of the energy necessary for channel opening, whereas VS of domain I has smaller contribution and input of voltage sensor of domain IV is negligible [190].

.

10.2 Voltage Dependent Inactivation

The channels activity is controlled by self-regulatory and extrinsic mechanisms that tune their action.

The excess of calcium influx is toxic, the entry of the Ca^{2+} into the cell is tightly regulated [61]. Hence, CaV possess self-regulatory and extrinsic mechanisms that permit them to tune their behavior in response to activity. This mechanism include voltage-dependent inactivation (VDI), calcium-dependent inactivation (CDI) and calcium-dependent facilitation (CDF) [45]. Perturbations in CDI lead to such diseases as authism [191] blindness [192] and cardiac arrhythmias, underlying importance of this process [156, 193].

Channels may inactivate from both open and closed states. Open-state inactivation occurs at strongly depolarized membrane potentials, and closed-stated inactivation mainly during the hyperpolarization [194]. It is also distinguished between voltage-dependent (VDI) and calcium-dependent inactivation (CDI). VDI is characterized by a slow and CDI by a fast time constant [195].

The Ca^{2+}-dependent inactivation is mediated by binding of calmodulin to the carboxy-terminal tail of L-type calcium channels [196]. Neely et al. showed that CDI does not depend on channel density, increases with Ca^{2+} current amplitudes and is faster at more negative potentials [126].

The molecular events during CDI are poorly understood. However, even in the absence of the auxillary subunits, calcium channels inactivate [79, 197]. Therefore, VDI should be initiated in the a1 pore-forming subunit.

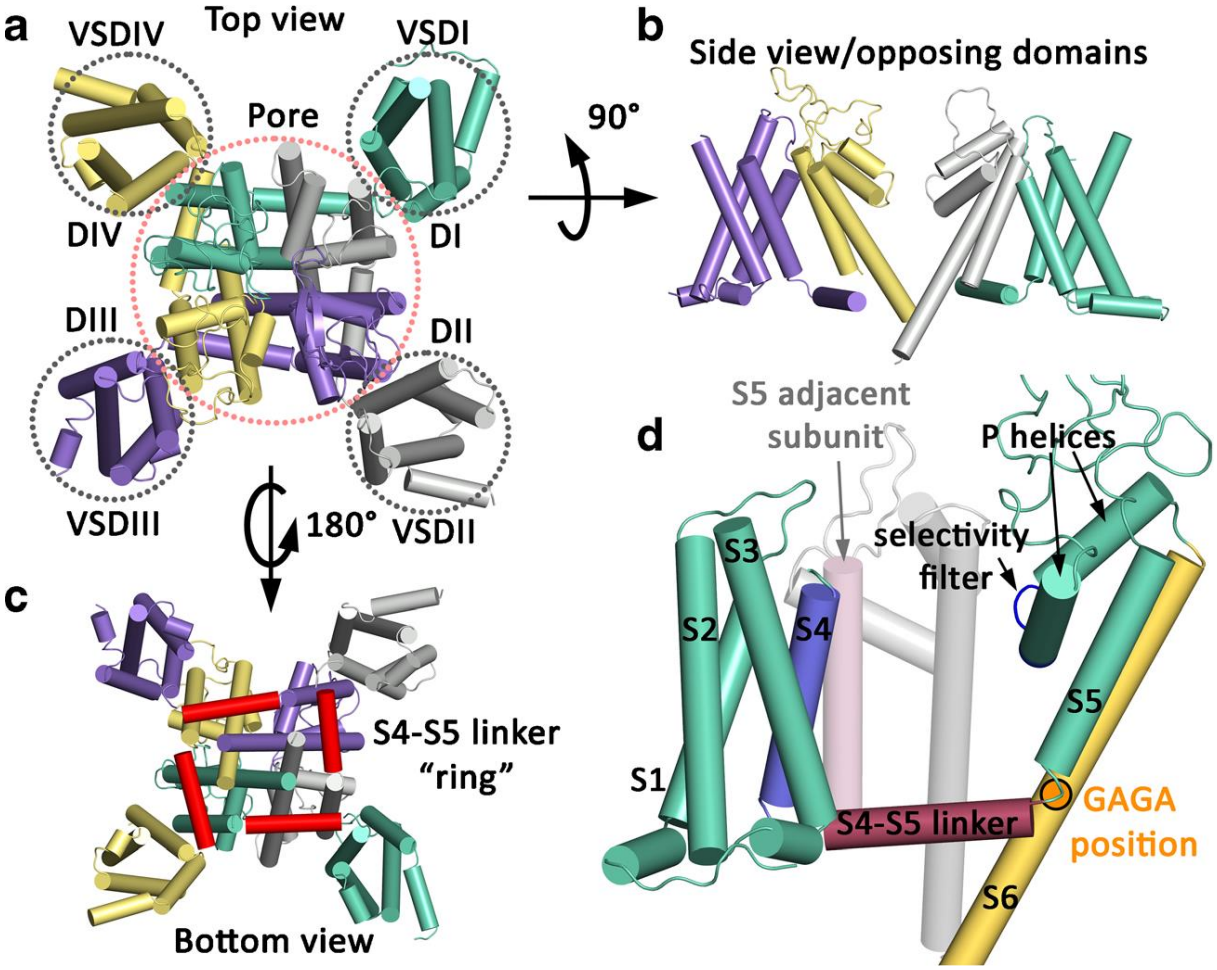


Figure 7.

Model of a CaV1.2 α1 subunit (based on the cryo-EM structure of CaV1.1 by Wu et al. [38, 206]). The helices are represented as cylinders. Domains I to IV are shown in green, gray, purple, and yellow, respectively. a The top view arrangement of the channel with the voltage-sensing domains (VSDI to VSDIV) and pore domain. B The side view shows the structural elements of opposing domains. The bundle-crossing region at the lower third of the S6 segments forms the activation gate. c The bottom view with a highlight on the S4–S5 linker ring (in red). The S4–S5 linker helices run in parallel to the intracellular side of the membrane. d One domain of the α subunit of the voltage-gated calcium channel. S1 to S3 (green) and S4 (blue) represent the voltage sensing domain. Segment S5, the P-helices (green), the selectivity filter (dark blue), and the S6 (yellow) form the pore domain. S4 is connected to the S5 via the S4–S5 – S5 linker (red). The S4 is further in close proximity to the S5 of the adjacent subunit (light pink). The S6 as well as the P-helices of the adjacent subunit are shown in light

gray. The G/A/G/A position is highlighted in orange , close to the loop between the S4–S5 linker and the S5 helix. Figure modified from Hering et al. [5].

Several groups have shown that certain point mutations in C-terminus, the I–II linker and the domain III and IV S6 regions, can dramatically affect inactivation kinetics [59, 79, 215-217].

Sometimes a single amino acid substitution is sufficient to abolish or to speed inactivation [217]. An insertion of a single valine in the I–II linker converted Q-type Ca^{2+} channel into non-inactivating P-type channel [218].

Spaetgens and Zamponi studied chimeras of channels that undergo slowly inactivation and channels that have rapid inactivation. They showed the contribution of all four transmembrane domains to the voltage dependence of inactivation. with Domains II and III mediated the bulk of the effects, whereas II, III and IV determined the rates of inactivation [219].

Armstrong et al. explained the fast inactivation mechanism of voltage-gated channels by so called “Ball and Chain“ mechanism [207]. They suggested that a short sequence of aminoacids („ball“) occludes the channel pore by an electrostatic binding. The similar mechanism was proposed also for voltage-gated potassium channels [208, 209].

Based on this model Stotz and colleagues proposed a similar mechanism of inactivation for calcium channels. In this model the I–II linker region could form a physical pore plug and dock to the S6 segments of domains II and III [210].

Another possible model for inactivation involves the pore collapse mediated inactivation by the S6 segments in domains II and III [200].

Stotz et al. investigated inactivation process in CaV channel in detail and proposed hinged lid mechanism of inactivation. They used chimeras of CaV1.2 (slow inactivating) and CaV2.3 (fast inactivating) and proposed a model in which the I-II linker docks at the domain II and III S6 regions, blocking the channel pore [79].

Marksteiner et al. found inactivation determinants of CaV2.1 in segment IIIS6. M1510I, F1511A slowed the I_{Ba} decay and V1512A significantly affected the inactivation time course at -20 mV [211].

However, several studies have shown, that other S6 may be involved in the channel inactivation. For example, Berjukow et al. discovered two aminoacids in IVS6 that affect inactivation development in CaV2.1 [212]. Stotz and Zamponi found that substitution of F823 in IIS6 of CaV1.2 by bulky aminoacids slows inactivation [213].

Recently Abderemane-Ali et al. [214] showed that selectivity filter controls CDI in CaV1.2 channel, beside the known regulatory elements [238] that were previously identified at the C-terminus [239]. Abderemane-Ali et al. introduced single point mutations (neutralized aspartate) in the selectivity filter and observed a drastically reduced CDI [214].

There are two proposed mechanisms for VDI:

i) The first possible mechanism is that inactivation is initiated by the opening of the activation gates due to allosteric interactions within the IIS6 segment.

ii) The second mechanism assumed that activation and inactivation are initiated by the voltage sensor movement.

VSs and S5 helices are connected via the S4–S5 linker (see Figure 7 c,d) - a helix which runs parallel to the intracellular side of the membrane and almost surrounds the pore domain at its intracellular side (see Figure 7 c). Each voltage-sensing domain is adjacent to the neighboring pore domain (e.g. see [198]), with the VS of one domain forming hydrophobic interactions with the S5 of the adjacent domain (Figure 7 d). This clockwise assembly not only allows the VSs to influence the gate of their own domains but potentially also the neighboring domains [5, 199].

Auxiliary subunits particularly beta subunits modulate the voltage dependence inactivation [200]. β3 or β1b typically accelerate inactivation, whereas rat β2a induces a dramatic slowing of inactivation, although β2a isoform isolated from other species doesn’t have this feature [79, 201-203]. The tethering of the β2a subunit to the plasma

membrane might restrict the mobility of the I–II linker, important for the channel inactivation, thus slowing inactivation kinetics [79].

β-subunits profoundly affect the voltage dependence of activation of HVA channels and generally enhance the activation and inactivation kinetics of CaV channels [204].

The binding affinity of several drugs, for instance DHPs, is higher in the inactivated than in other states [60, 205]

11 Aim of the study

Two positively charged amino acids arginine and lysine carry the primary gating charges on segments S4. Substitution of the positive charges to the neutral glutamine by site-directed mutagenesis should reduce the steepness of voltage-dependent gating and shift its position on the voltage axis [46]. Here, we made use of CaV1.2 constructs with fully or partially neutralized charges in S4 segments and „GAGA mutations" (a ring of alanines and glycines: G432W (IS6), A780T (IIS6), G1193T (IIIS6), A1503G (IVS6)) to understand individual roles of voltage sensors in CaV 1.2 gating (activation, deactivation and inactivation processes).

We aimed to answer following questions:

1. Which of the four domains is most crucial for channel opening?

2. How charge neutralisations of S4 segments affect kinetics of activation and inactivation?

3. Which of the four S4 segments has a key role in channel inactivation?

4. Is there a correlation between the number of S4 charges VSs and channel inactivation?

12 Materials and methods

12.1 Mutagenesis

Substitutions in S4 segments of the CaV1.2 α1-subunit (GenBank™ X15539) were introduced using the QuikChange® Lightning Site-Directed Mutagenesis Kit (Stratagene) with mutagenic primers according to the manufacturer's instructions. All constructs were checked by restriction site mapping and sequencing.

12.2 Cell culture and transient transfection

Human embryonic kidney (HEK293) tsA-201 cells were grown at 5% CO2 and 37°C to 80% confluence in Dulbecco's modified Eagle's/F-12 medium supplemented with 10% (v/v) fetal calf serum and 100 units/ml penicillin/streptomycin. Cells were split with accutase solution and plated on 35 mm Petri dishes (Falcon) at 60–80% confluence ~24 h before transfection. Subsequently, tsA-201 cells were co-transfected with cDNAs encoding WT or mutant CaV1.2 α1-subunits with auxiliary β3a (β2a for deactivation and GAGA mutants studies) as well as α2-δ1 [205] subunits and GFP to identify transfected cells.

The transfection of tsA-201 cells was performed using the TurboFect Transfection Reagent (Thermo Fisher Scientific) following standard protocols. HEK293 cells were used until passage number 26. No variation in channel gating related to different cell passage numbers was observed.

In order to avoid calcium-dependent inactivation, 20mM barium (5mM for deactivation and GAGA mutants studies) solutions were used as a charge carrier (see Andranovits et al. [6] and Beyl et al. [4] for details).

12.3 Ionic current recordings and data acquisition

Barium currents (IBa) through voltage-gated Ca^{2+} channels were recorded at 22–25°C by patch-clamp [32] using an Axopatch 200A patch clamp amplifier (Axon Instruments, Foster City) 24–48 h after transfection. To avoid calcium-dependent inactivation, barium was used as charge carrier. The extracellular bath solution (in mM: $BaCl_2$ 20, $MgCl_2$ 1, HEPES 10, choline-Cl 140) was titrated to pH 7.4 with sodium hydroxide. Patch pipettes with resistances of 1 to 4 MΩ were made from borosilicate glass (Clark Electromedical Instruments, UK) and filled with pipette solution (in mM: CsCl 145,

$MgCl_2$ 3, HEPES 10, EGTA 10), titrated to pH 7.25 with CsOH. All data were digitised using a DIGIDATA 1200 interface (Axon Instruments, Foster City), smoothed by means of a four-pole Bessel filter and saved to disc. 100-ms current traces were sampled at 10 kHz and filtered at 5 kHz. Leak currents were subtracted digitally using average values of scaled leakage currents elicited by a 10 mV hyperpolarizing pulse or electronically by means of an Axopatch 200 amplifier (Axon Instruments, Foster City). Series resistance and offset voltage were routinely compensated for. The pClamp software package (Version 10.0 Axon Instruments, Inc.) was used for data acquisition and preliminary analysis. Microcal Origin 7.0 was used for analysis and curve fitting.

12.4 Analysis of current kinetics

The voltage dependence of activation was determined from I-V curves that were fitted according to the following modified Boltzmann distribution:

$$I = \frac{G_{\max} \cdot (V - V_{rev})}{1 + \exp(\frac{V_m - V}{k_s})}$$

where V is membrane potential, I is peak current, G_{max} is maximum membrane conductance, V_{rev} is extrapolated reversal potential, V_m is voltage for half-maximal activation, and ks is slope factor. The time course of current activation, deactivation and inactivation were fitted to a monoexponential function over 3000 ms:

$$I(t) = A \cdot \exp\left(-t / \tau_{inact}\right) + C$$

where I(t) is current at time t; A is the amplitude coefficient; $\tau_{inact.}$ is the time constant; and C the steady-state current. Data are given as mean ± S.E.

The voltage dependence of IBa inactivation (inactivation curve) was measured using a double-pulse protocol to account for run-down [67]. The pulse sequence was applied every 60s from a holding potential of −110 mV, length of conditioning pulse 3000 ms :

Inactivation curves were drawn according to a Boltzmann equation:

$$h = h_{SS} + \frac{1 - h_{SS}}{1 + \exp\left(\frac{V - V_{0.5,inact}}{k_{inact}}\right)}$$

where V is membrane potential, $V_{0.5}$,inact is midpoint voltage, k_{inact} is the slope factor, and h_{ss} is the fraction of non-inactivating current. Data are given as mean ± S.E. Statistical significance was assessed with the Student's unpaired t test.

13 Results

During this thesis project I investigated the role of S4 charges in CaV1.2 gating.

Positively charged amino acids: arginine (R) and lysine (K) were step-by-step replaced by glutamines in down-stream direction [6] (see Figure 8).

Previously Beyl et al. reported that complete neutralization of positive amino acids in voltage-sensing domains of IS4-IVS4 segments resulted in only one functional construct of CaV1.2 – IIS4N [220]. Therefore instead of the completely neutralized VSs I studied the individual role of VSs with a 'maximal possible' number of neutralized charges.

In the second part of the study I used slowly-gating pore (GAGA) mutants as tools to analyze the domain-specific impact of S4 segments on both CaV1.2 deactivation and activation.

For inactivation and activation studies all mutant CaV1.2 α1 subunits were co-expressed with the β3 subunit, known to promote channel inactivation [221]. Deactivation and activation studies on GAGA-mutants were performed on the channel mutants expressed with β2 subunit.

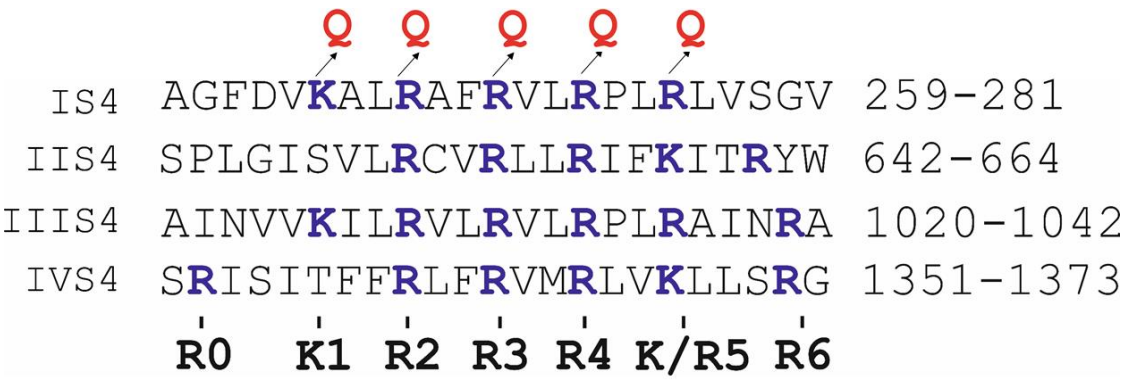


Figure 8.

Alignments of S4 segments . Charged residues are shown in *blue.* Arrows symbolize substitution of lysines (K) and arginines (R) to glutamines (Q).

13.1 Principal role of IS4 in activation

Replacement of the outermost charged residue in IS4 by glutamine shifted the steady-state activation curve significantly rightwards (V0.5,act (IS4(K1Q))= 13.2±0.5 mV, V0.5,act(WT) = 1.8±0.5 mV, Figure 9a, Table 3) [6].

Mutant with two outermost neutralized charges (IS4(K1Q/R2Q)) moved activation curve slightly to the more depolarized voltages (V0.5,act (IS4(K1Q/R2Q))= 7.1 ± 0.8 mV vs V0.5,act(WT) = 1.8±0.5 mV, Figure 9a, Table 3) [6].

Mutants lacking three and four charges activated at significantly more negative voltages (V0.5,act(IS4(K1Q/R2Q/R3Q)) = -11.9±0.5 mV, V0.5,act (IS4(K1Q/R2Q/R3Q/R4Q)) = -20.9±0.3 mV ; Fig 9a, Table 3) [6].

Interestingly, all IS4 mutants except a single point mutation (K1Q) induced a significant reduction of the slope of the Boltzmann curve (from kact = 6.6 ± 0.3 in WT to 8.8 ± 0.3 mV in IS4(K1Q/R2Q/R3Q/R4Q), to 7.3 ± 0.3 mV IS4(K1Q/R2Q/R3Q) and to 9.4 ± 0.8 in IS4(K1Q/R2Q), see , Figure 10, Table 3) [6].

A similar study was performed with segment IIS4: Neutralization of all IIS4 charges (IIS4(R2Q/R3Q/R4Q/K5Q/R6Q)) partially neutralized IIS4 (IIS4(R2Q/R3Q/R4Q/K5Q)) and two single point mutants (IIS4(R2Q) and IIS4(R6Q)) induced minor shifts (less than 10 mV) of the activation curves (Figure 9b) and did not affect current kinetics (Figure 18 a). Unlike the effect in IS4 mutants only one neutralization of the upper positive charge in the IIS4 (mutant IIS4(R2Q)) significantly affected the slope of the activation curve (Figure 10 and Table 3), possibly meaning the importance of this charge in the activation process [6].

Transfection with cDNA of fully neutralized construct IIIS4(K1Q/R2Q/R3Q/R4Q/R5Q) did not result in functional channels [4]. Mutants IIIS4(K1Q/R2Q/R3Q/R4Q) and IIIS4(K1Q) were functional, but none of them induced a significant shift of the activation curve (Fig 9c). The slope of the Boltzmann curve only of single-point mutant IIIS4(K1Q) was significantly reduced compared to wild-type channel (Figure 10, Table 3) [6].

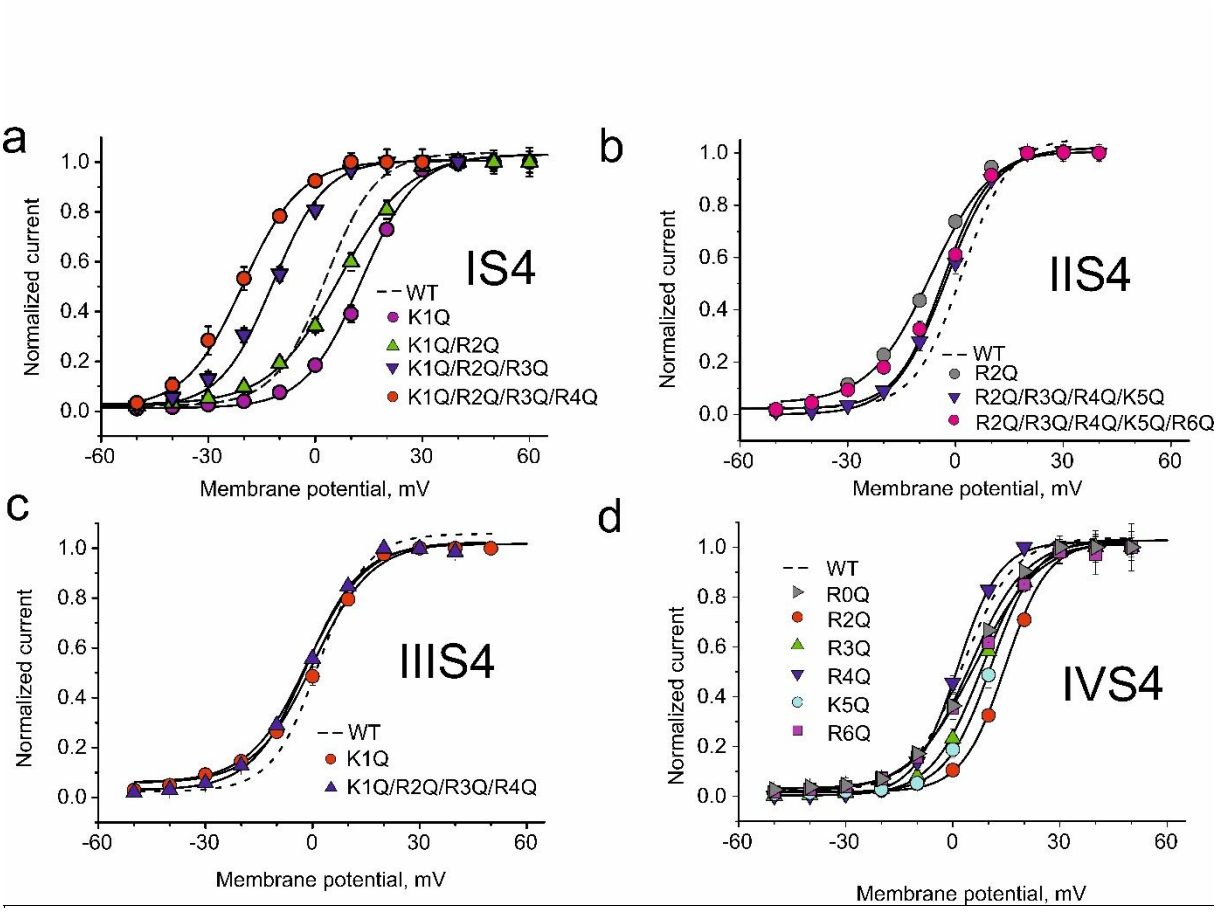


Figure 9.

Neutralisation of charges in segments IS4 has significant effect on steady-state activation.

Steady-state activation of CaV1.2 mutants with gradually neutralized IS4 (a), IIS4 (b), IIIS4 (c) and IVS4 charges (d). Figure modified from Andranovits et al. [6]

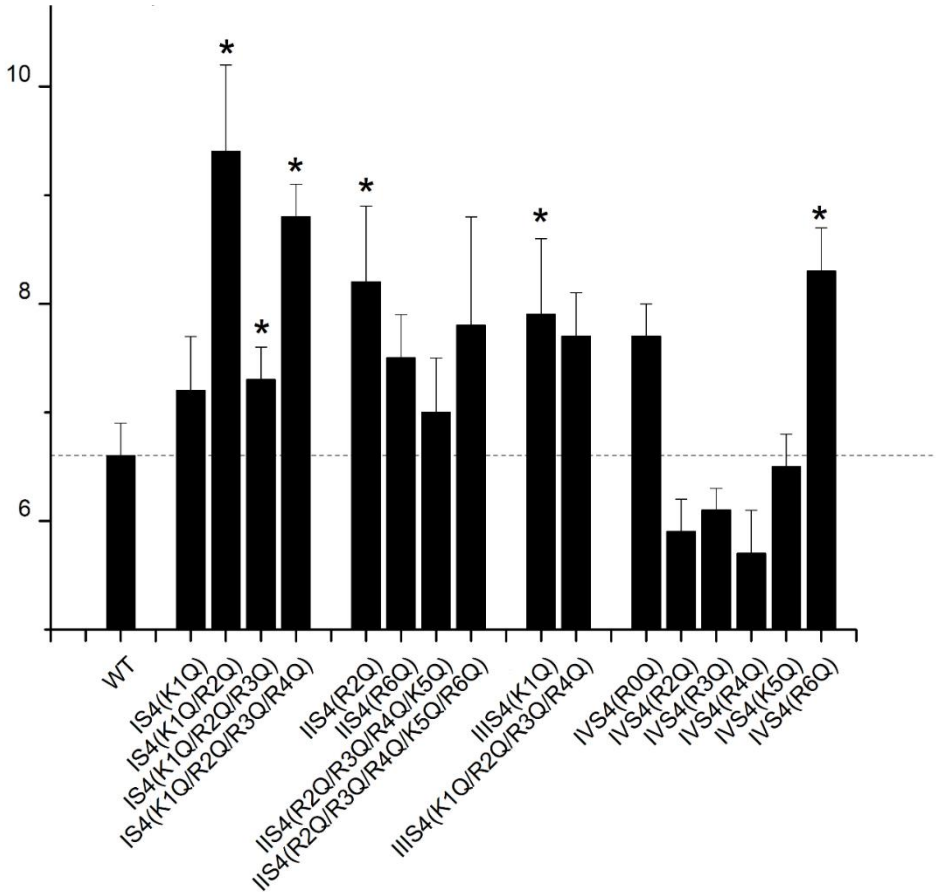


Figure 10.

Neutralisations in IS4–IVS4 differently affect the slope of the CaV1.2 activation curve. Compared to wild-type CaV1.2, slope factors of the activation curves were significantly (*$p < 0.05$) increased by most of IS4 mutants. Only single point mutations of upper charges in IIS4 and IIIS4, and lower charge in IVS4 affected the slope.

Neutralisation of either five (R2–R6), the upper four (R3–R6), the upper three (R4–R6) or even two (R2 and R3, Figure 8) charges of IVS4 did not result in conducting channel constructs [4].

Therefore I investigated the individual contributions of each of the six IVS4 charges (Figure 8). Figure 9d illustrates the corresponding steady-state activation curves. Only single point mutations IVS4(R2Q) and IVS4(K5Q) induced significant rightward shifts of activation curves towards more depolarized voltages ($\Delta V_{0.5,act.}$(IVS4(R2Q))=15.0±0.4; $\Delta V_{0.5,\ act}$(IVS4(K5Q))=8.9±0.3 , Figure 9d, Table 3).

CaV1.2 structure shows that R2 charge of IVS4 may interact with aspartic acid in IVS3 segment (D1327) (See Figure21) [6] . Interestingly, this negatively charged residue is highly conserved throughout the CaV family [149].

Costé de Bagneaux et al. [149] hypothesized that interaction between R2 and D1327 may determine the voltage dependence of activation in CaV1.2.

Other mutations induced just small or negligible changes. The effects of IVS4 charge neutralisations on the slope factor of the activation curve are illustrated in Figure 10. Only neutralization of the uppermost charge in IVS4 (IVS4(R6Q)) reduced the slope of the activation curve (from k_{act} = 6.6 ± 0.3 to 8.3 ± 0.4 mV, see , Figure 10, Table 3) [6].

Furthermore we have studied combinations of VS mutants with slowly gating pore (S6) mutants : G432W, A780T, G1193T, A1503G (see Table 2). Activation/deactivation of "GAGA-mutants" is decelerated (Figure11B) and the activation curves of these constructs are shifted to the left compared to WT (Figure11A) [4].

Table 2. Midpoints and slope factors (k) of the activation curves of GAGA-mutants and combinations of GAGA mutants with S4 neutralizations. [a]Data from [1]. Table modified from Beyl et al. [4]

Mutant	$V_{0.5}$, mV	$K_{act,}$ mV
WT	-18.6 ± 0.8 (n=7)	5.9 ± 0.9
G432W[a]	−33.7 ± 0.6 (8)	4.7 ± 0.4
A780T[a]	−44.0 ± 0.6 (5)	5.1 ± 0.6
G1193T[a]	−49.8 ± 1.0 (7)	5.1 ± 0.6
A1503G[a]	−41.4 ± 0.8 (5)	5.8 ± 0.5
IS4 neutralizations		
G432W+IS4(K1Q/R2Q/R3Q/R4Q)	No detectable current	

A780T+IS4(K1Q/R2Q/R3Q/R4Q)	−42.7 ± 1.1 (4)	11.9 ± 1.0
G1193T+IS4(K1Q/R2Q/R3Q/R4Q)	No detectable current	
A1503G+IS4(K1Q/R2Q/R3Q/R4Q)	−41.1 ± 0.6 (5)	8.7 ± 0.5
IIS4 neutralizations		
G432W+IIS4(R2Q/R3Q/R4Q/K5Q)	−31.0 ± 0.6 (5)	8.4 ± 0.8
A780T+ IIS4(R2Q/R3Q/R4Q/K5Q)	−33.6 ± 0.6 (4)	6.3 ± 0.3
G1193T+ IIS4(R2Q/R3Q/R4Q/K5Q)	−38.0 ± 0.8 (5)	6.1 ± 0.6
A1503G+ IIS4(R2Q/R3Q/R4Q/K5Q)	−25.3 ± 1.0 (6)	7.7 ± 0.6
IIIS4 neutralizations		
A780T+IIIS4(K1Q/R2Q/R3Q/R4Q)	−43.6 ± 0.6	9.3 ± 0.4
G1193T+ IIIS4(K1Q/R2Q/R3Q/R4Q)	−41.8 ± 0.6	8.2 ± 0.6

Combination of IS4(K1Q/R2Q/R3Q/R4Q) with A780T significantly increased the slope of the activation curve (from 5.1 ± 0.6 to 11.9 ± 1.0 mV, $p < 0.05$, Figure15c) without significantly shifting the midpoint of the curves [4].

The IS4(K1Q/R2Q/R3Q/R4Q) was studied in combination with another GAGA mutant: A1503G. This combination increased the slope factor from 5.8±0.5 to 8.7±0.5 mV, and like IS4(K1Q/R2Q/R3Q/R4Q) with A780T did not affect the position of the activation curve (Table 2, Figure12 A). Two other mutants G432W+IS4(K1Q/R2Q/R3Q/R4Q) and G1193T+ IS4(K1Q/R2Q/R3Q/R4Q) did not result in detectable currents [4].

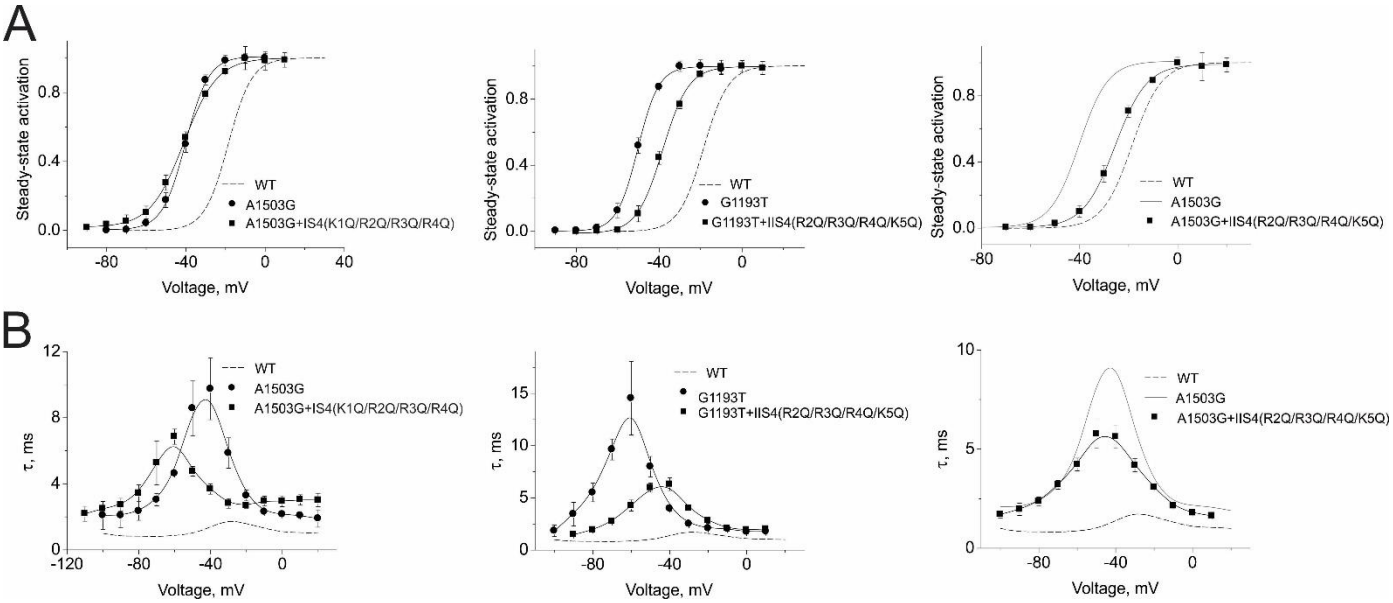


Figure 11.

Modulation of gating in GAGA-mutants by single charged IS4 or IIS4.

A, averaged activation curves of WT, GAGA-mutants (A1503G and G1193T) and corresponding combinations with single charged IS4 (IS4(K1Q/R2Q/R3Q/R4Q)) or IIS4 (IIS4(R2Q/R3Q/R4Q/K5Q)). Neutralisation of IS4 caused shift of activation curve (*left*), while IIS4 neutralisation caused the rightward shift of activation. Figure modified from Beyl et al. [4]

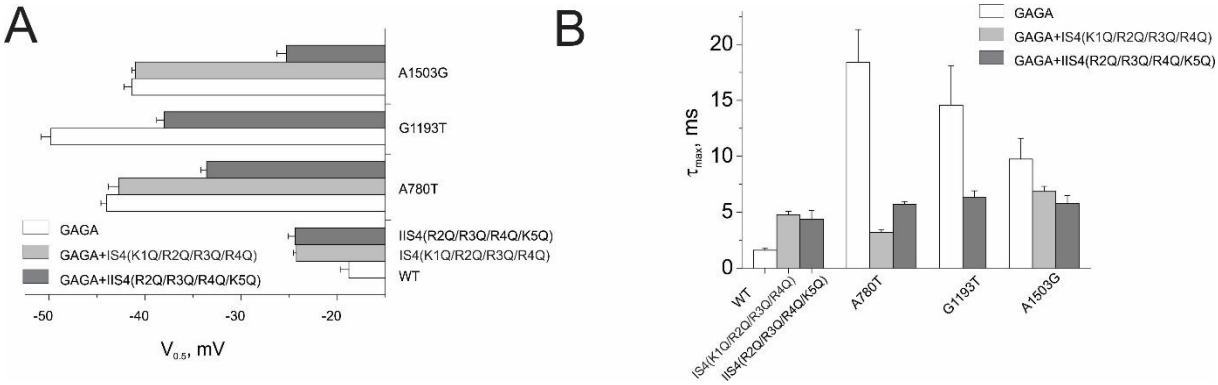


Figure 12.

Effect of charge neutralization in IS4 and IIS4 on CaV1.2 gating

A , Half-activation voltage of studied constructs. Significant shift of activation caused by GAGA mutations (white bars) is partially rescued by charge neutralisations in IIS4 (dark bars) but not IS4 neutralisation (light bars). B, τ_{max} of studied constructs. Voltage-sensor neutralisations in IS4 or IIS4 accelerate the “slowly” gating GAGA mutants. Figure modified from Beyl et al. [4]

A contrasting picture was observed for GAGA mutation A780T with IIS4N carrying only a single arginine at the lowest position. IIS4(R2Q/R3Q/R4Q/K5Q) shifted the activation

curve of A780T by +10.3 ± 0.8 mV to the right (Figure 15e) without, however, affecting the slope of the curve (Figure 15e, Table 2) [4].

Figure15f illustrates the acceleration of current kinetics of A780T caused by IIS4 neutralisation (IIS4(R2Q/R3Q/R4Q/K5Q)). A similar observation was made for combinations of the same mutant with three other pore mutations (G432W(IS6), G1193T (IIIS6), A1503G (IVS6); see Figs.12B) [4].

The observed shifts of the activation curve compared to corresponding GAGA-mutants ranged between 2.7 ± 0.8 mV (G432W +IIS4(R2Q/R3Q/R4Q/K5Q)) and 16.1±1.3 mV (A1503G+IIS4(R2Q/R3Q/R4Q/K5Q)). No significant effect of a partially charged IIS4 on the slope of the activation curve was observed for most of these constructs (Table 2). In some pore mutants, charge neutralisations in segment IIS4 reduced, however, the activation slope (e.g. G432W+ IIS4(R2Q/R3Q/R4Q/K5Q) and A780T+IIS4(K5Q)) suggesting peculiarities of the pore–S4 interplay in these constructs [4].

Two combinations of maximally neutralized IIIS4 with GAGA-mutations were studied. A780T+IIIS4(K1Q/R2Q/R3Q/R4Q) did not shift the activation curve compared to A780T mutant (-43.66±0.6 mV against -44.0±0.6 mV correspondingly) [4].

However, combination of IIIS4(K1Q/R2Q/R3Q/R4Q) with G1193T shifted the activation curve slightly to the more depolarized direction (-49.8±1.0 mV vs -41.8±0.6 mV). Interestingly, both mutants significantly increased the slope of the activation curve. Combination with A780T from 5.1±0.6 to 9.3±0.4 mV and with G1193T to 8.2±0.6 from 5.1±0.6 mV (Table 2) [4].

13.2 IS4 and IIIS4 stabilize the open channel pore

We investigated the role of VSs in deactivation of CaV1.2 by studying the effects of neutralized VS of different domains on deactivation kinetics.

By first glance charge neutralization in IS4–IVS4 did not affect current kinetics of deactivation which prevented conclusions about S4-mediated stabilizations of open/closed channel conformation (See Figure 14) [4]. Therefore, in order to further

elucidate the individual effects of segments IS4 and IIIS4 on deactivation, we used as a tool GAGA mutations with decelerated deactivation [4].

A removal of four out of five charges from IS4 reduced the time constant of activation/deactivation at the peak of the bell-shaped curve from 18.4 ± 2.9 ms in A780T to 3.1 ± 0.2 ms in A780T+IS4(K1Q/R2Q/R3Q/R4Q) (Figure15 d) [4].

Acceleration of tail currents by introduction of IS4(K1Q/R2Q/R3Q/R4Q) into A780T (See Figure15 b) underlines an important role of IS4 charges in stabilisation of the open channel pore [4].

Neutralisation of IIIS4 charges on pore mutant A780T substantially accelerated deactivation (from τ_{max}=18.4±2.9 in A780T to 5.2±0.5 ms in A780T+ IIIS4(K1Q/R2Q/R3Q/R4Q)), highlighting a role of this segment in stabilization of the open channel state (Fig 13B) [4].

13.3 Gradual neutralisation of IS4 charges enhanced voltage-dependent inactivation of CaV1.2 channel

Gradual neutralization of positively charged amino acids shifted the steady-state inactivation curve to more depolarized voltages. More charges were neutralized in IS4 segment, earlier started inactivation [6].

Replacement of the outermost charge in IS4 segment by uncharged glutamine (mutant IS4(K1Q)) induced a statistically non-significant rightward shift of the steady-state inactivation curve ($\Delta V_{0.5,inact}$(IS4(K1Q))= -13.2±3.5 mV *vs*. $\Delta V_{0.5,inact}$(WT)=-18.3±1.1 mV, Figure16c, Table 3) and neutralisation of the two upper charges IS4(K1Q/R2Q) resulted in a left shift compared to IS4(K1Q): $V_{0.5,inact}$ (IS4(K1Q/R2Q))= -20.3±1.2 mV. Neutralisation of three IS4(K1Q/R2Q/R3Q) or four charges IS4(K1Q/R2Q/R3Q/R4Q) shifted of the inactivation curve further into the hyperpolarising direction with midpoint voltages of $V_{0.5,inact}$ (IS4(K1Q/R2Q/R3Q)) =-38.1±0.8 mV and $V_{0.5,inact}$(IS4(K1Q/R2Q/R3Q/R4Q)) = -45.0±0.7 mV (Figure16c) [6].

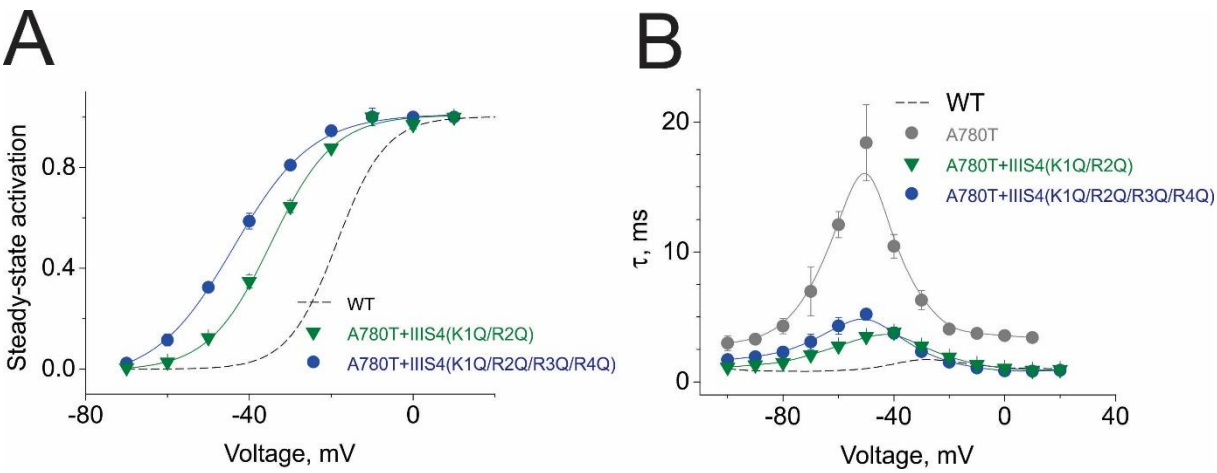


Figure 13.

Neutralisation of IIIS4 charges affects gating of A780T.

A, Averaged activation curves of WT and constructs A780T+IIIS4(K1Q/R2Q) and A780T+IIIS4(K1Q/R2Q/R3Q/R4Q).
B, Voltage-dependent time constants of channel activation/deactivation of WT, A780T, A780T+IIIS4(K1Q/R2Q) and A780T+IIIS4(K1Q/R2Q/R3Q/R4Q).

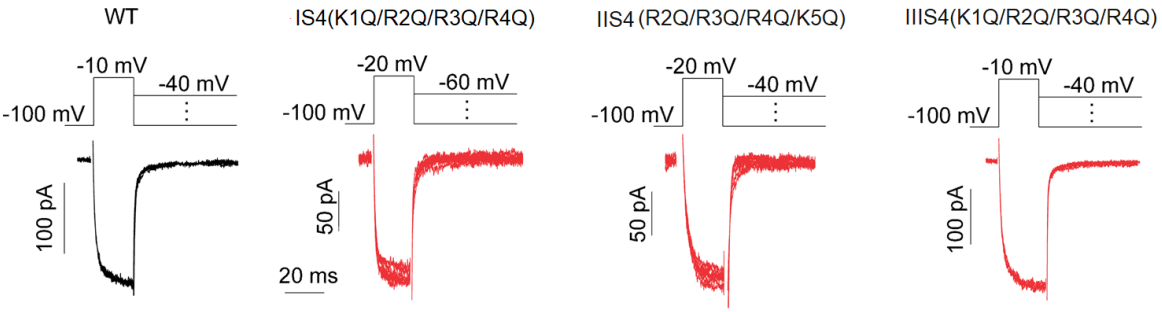


Figure 14.

Modulation of CaV1.2 deactivation by S4 charge neutralisations.

Tail currents of IBa through wild-type and mutant channel constructs with partially neutralized S4 segments (IS4(K1Q/R2Q/R3Q/R4Q), IIS4N(R2Q/R3Q/R4Q/K5Q), IIIS4N(K1Q/R2Q/R3Q/R4Q)). The deactivation was measured by applying the voltage steps to different potentials after a short (20 ms) activating pulse (b). Note that neutralization of S4 charges has minor effects on deactivation kinetics of CaV1.2. Figure modified from Beyl et al. [4]

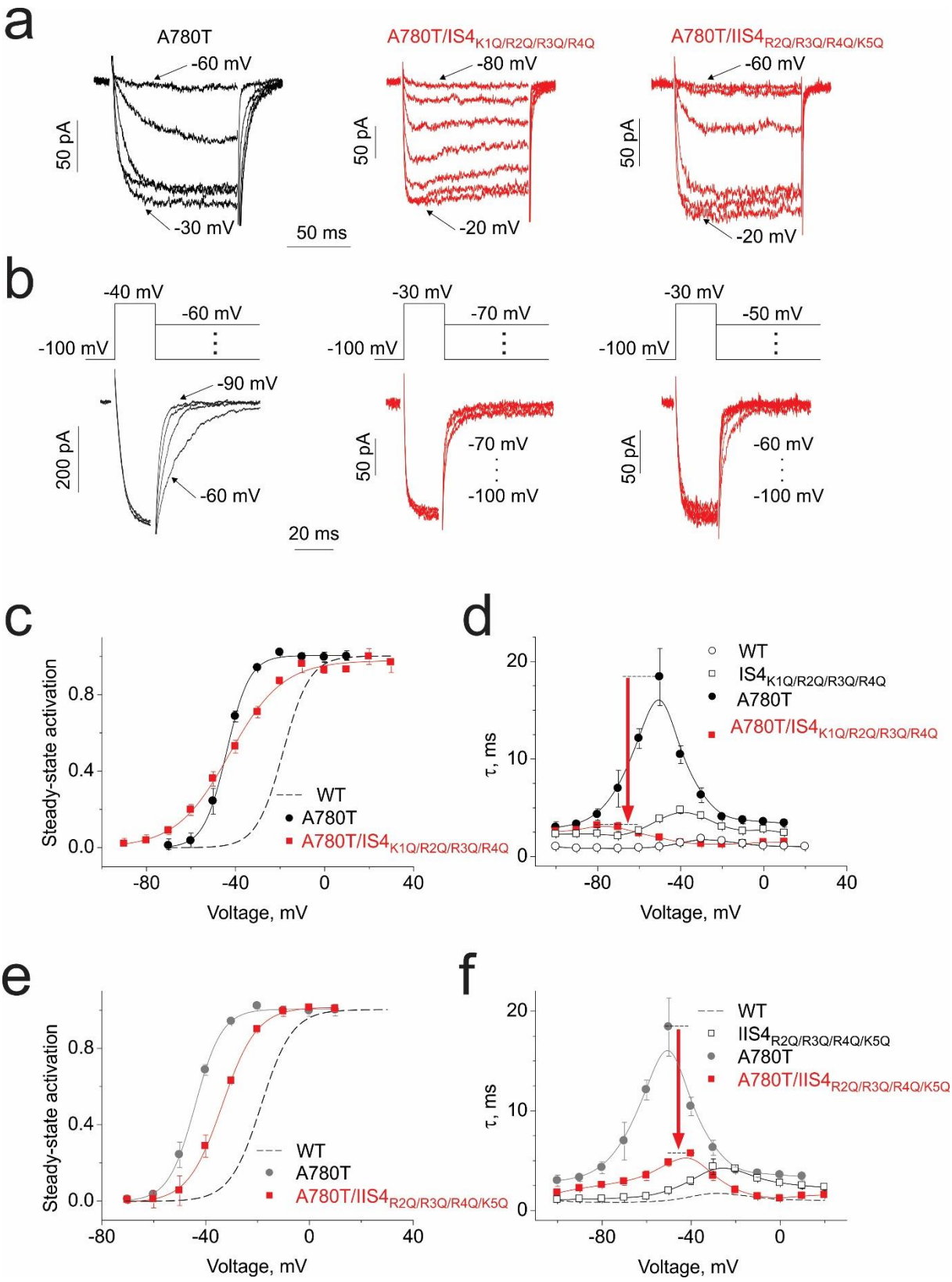


Figure 15.

Modulation of pore mutant A780T by IS4 and IIS4 carrying a single charge (IS4(K1Q/R2Q/R3Q/R4Q) and IIS4N(R2Q/R3Q/R4Q/K5Q)). Activation (a) and deactivation (b, tail current) of IBa through pore mutant A780T and corresponding constructs with partially neutralized segment IS4(K1Q/R2Q/R3Q/R4Q), four out of five

IS4 charges are substituted by glutamines) and IIIS4N steps (R2Q/R3Q/R4Q/K5Q), four out of five IIS4 charges are substituted by glutamines). The deactivation was measured by applying the voltage to different potentials after a short (20 ms) activating pulse (b, voltage protocol above current traces). Partial neutralization of IS4 or IIS4 charges caused a significant acceleration of current kinetics of the slowly gating A780T (constructs A780T+IS4(K1Q/R2Q/R3Q/R4Q) and A780T+IIS4N(R2Q/R3Q/R4Q/K5Q), arrows on d and f. c, e Averaged activation curves of WT, A780T, A780T+IS4(K1Q/R2Q/R3Q/R4Q) and A780T+IIS4N(R2Q/R3Q/R4Q/K5Q) channels. The slope of A780T +IS4(K1Q/R2Q/R3Q/R4Q) was significantly reduced (from k_{act} = 5.1 ± 0.6 mV in A780T to k_{act} = 11.9 ± 1.0 mV in A780T+ IS4(K1Q/R2Q/R3Q/R4Q)). The slope of A780T/IIS4N(R2Q/R3Q/R4Q/K5Q) activation curve was not changed while the activation curve was shifted by +10.3 ± 0.8 mV. d, f Voltage-dependent time constants of channel activation/deactivation. Red arrows highlight the acceleration of current kinetics when A780T was combined with a 'neutralized' S4 segment (Figure from Beyl et al. [4]).

Interestingly, charge neutralisation gradually reduced the slope factor (k_{inact}) of the inactivation curves compared to WT: $k_{inact.}$(IS4(K1Q/R2Q/R3Q/R4Q))= 6.2±0.7 mV and k_{inact} (IS4(K1Q/R2Q/R3Q))= 8.2±0.6 mV vs. k_{inact} (WT)= 14.1±0.8 mV, see Figures 16c and 19d. Transfection of cells with cDNA of a construct where all IS4 charges were neutralized did not result in functional channels [6].

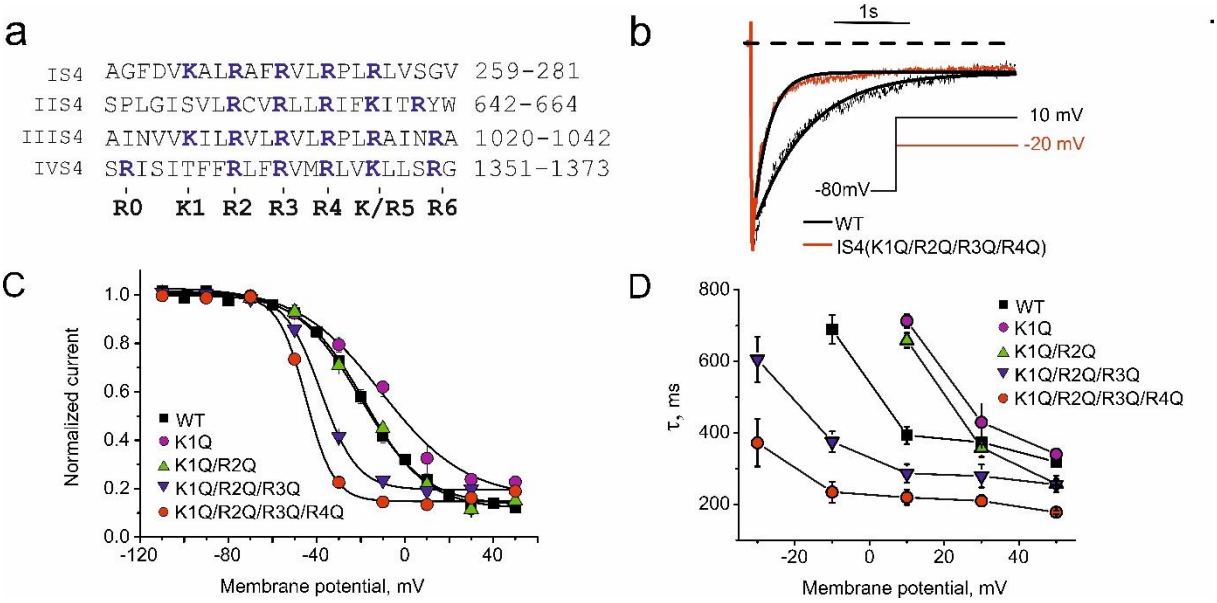


Figure 16.

a, Neutralization of segment IS4 modulates CaV1.2 inactivation. Alignment of CaV1.2 segments IS4-IVS4. Charged residues are highlighted in blue. **b**, Superimposed typical normalized I_{Ba} through WT and mutant IS4(K1Q/R2Q/R3Q/R4Q). I_{Ba} through WT and quadruple mutant IS4(K1Q/R2Q/R3Q/R4Q) during 3 second depolarizations from – 80

mV to the voltages of the maximum of the current-voltage relationship (WT: 10 mV; IS4(K1Q/R2Q/R3Q/R4Q): -20 mV). Note the faster development of inactivation in IS4(K1Q/R2Q/R3Q/R4Q). Current decay was fitted to a monoexponential function yielding time constants of τ_{inact}(WT) = 393±24 ms and $\tau_{inact.}$(IS4(K1Q/R2Q/R3Q/R4Q)) = 235±29 ms, respectively (see Methods). Solid lines represent the fitted function. **c**, Steady-state inactivation curves of WT and the indicated IS4 mutants. Voltages of half-maximal inactivation ($V_{0.5,inact}$) where -18.3±1.1 mV (WT), -13.2±3.5 mV (IS4(K1Q)), -20.3±1.2 mV (IS4(K1Q/R2Q)), -38.1±0.8 mV ((IS4(K1Q/R2Q/R3Q)), and -45.0±0.7 mV ((IS4(K1Q/R2Q/R3Q/R4Q)). **d**, Inactivation time constants (τ_{inact}) at different voltages were obtained by fitting the I_{Ba} decay over an interval of 3000 ms by a mono-exponential function. Time constants for WT and the indicated IS4 mutants are plotted as function of the membrane potential [6]. Figure modified from Andranovits et al.[6]

Neutralisations of charges in segment IS4 did not only affect the steepness and position of the steady-state inactivation curves but also changed kinetics of the current inactivation. Figure17 illustrates accelerated inactivation kinetics of IS4(K1Q/R2Q/R3Q/R4Q) compared to WT (see inactivation time constants of this and other mutants in Figure19d).

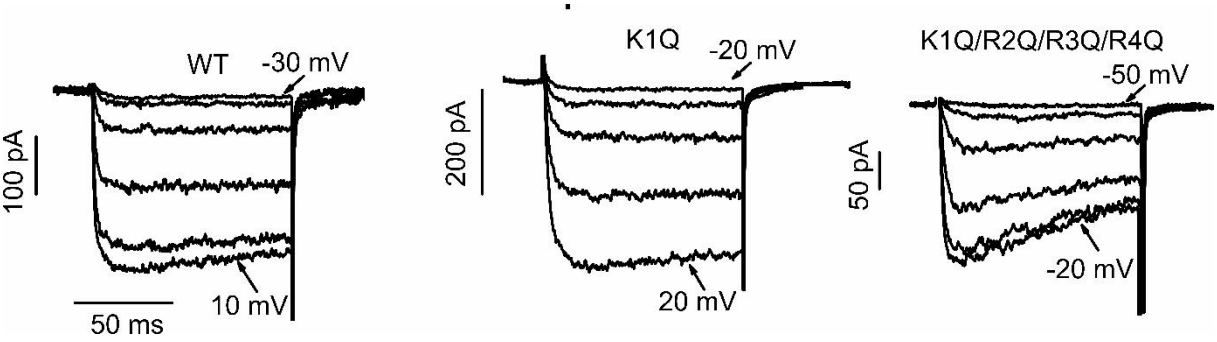


Figure 17.

Activation currents of IBa through WT and mutant channel constructs with partially neutralized S4 segments (IS4(K1Q) and IS4(K1Q/R2Q/R3Q/R4Q)). Currents were recorded by applying a 100-ms pulse from holding potential (−80 mV) with 10 mV steps (WT −30 mV − +10 mV, K1Q −20 mV − +20 mV, K1Q/R2Q/R3Q/R4Q −50 mV − −20 mV). IS4(K1Q/R2Q/R3Q/R4Q) activates at more negative voltages than IS4(K1Q/R2Q/R3Q) and WT while IS4(K1Q) activates at more positive voltages (Table 3). Charge neutralization in IS4 (K1Q/R2Q/R3Q/R4Q) notably accelerates inactivation. Compare typical current recordings of WT (upper panel) with mutants K1Q (middle panel) and quadruple mutant IS4(K1Q/R2Q/R3Q/R4Q) (lower panel). Figure modified from Andranovits et al. [6]

A highly significant ($p<0.01$) linear correlation between the voltages of half maximal inactivation ($V_{0.5, inact}$) and activation ($V_{0.5, act}$, Figure 22) with r= 0.95 was observed [6].

Table 3. Midpoint voltages and slope factors (k) of the activation and inactivation curves. Numbers of experiments are indicated in parentheses. From Andranovits et al. [6]

Mutant	$V_{0.5\ act}$, mV	K_{act} , mV	$V_{0.5\ inact}$, mV	K_{inact} , mV
WT	1.8±0.5 (n=13)	6.6±0.3	-18.3±1.1 (n=10)	14.1±0.8
IS4 mutants				
K1Q	13.2±0.5 (8)	7.2±0.5	-13.2±3.5 (3)	17.4±3.5
K1Q/R2Q	7.1±0.8 (6)	9.4±0.8	-20.3±1.2 (3)	14.7±1.4
K1Q/R2Q/R3Q	-11.9±0.5 (10)	7.3±0.3	-38.1±0.8 (4)	8.2±0.6
K1Q/R2Q/R3Q/R4Q	-20.9±0.3 (10)	8.8±0.3	-45.0±0.7 (6)	6.2±0.7
IIS4 mutants				
R2Q	-7.8±0.7 (3)	8.2±0.7	-22.3±3.6 (3)	13.9±1.9
R6Q	-4.7±0.4 (3)	7.5±0.4	-29.7±1.0 (3)	12.6±0.7
R2Q/R3Q/R4Q/K5Q	-2.2±0.5 (3)	7.0±0.5	-27.8±1.6 (3)	13.8±1.0
R2Q/R3Q/R4Q/K5Q /R6Q	-3.3±1.1 (3)	7.8±1.0	23.0±1.3 (3)	15.4±1.2
IIIS4 mutants				
K1Q	0.7±0.8 (3)	7.9±0.7	-22.0±3.0 (3)	12.0±1.3
K1Q/R2Q/R3Q/R4Q	-1.8±0.6 (4)	7.7±0.4	-26.3±1.9 (4)	11.3±1.6
IVS4 mutants				
R0Q	5.1±0.3 (5)	7.7±0.3	-17.7±2.5 (5)	13.7±2.3
R2Q	15.0±0.4 (8)	5.9±0.3	-0.9±1.3 (3)	10.2±1.2
R3Q	6.5±0.3 (4)	6.1±0.2	-21.3±1.8 (3)	13.6±1.6
R4Q	0.7±0.6 (3)	5.7±0.4	-22.9±0.9 (3)	9.7±0.7
K5Q	8.9±0.3 (5)	6.5±0.3	-5.6±1.3 (3)	8.1±0.7
R6Q	5.6±0.4 (5)	8.3±0.4	-20.8±2.4 (3)	12.3±1.9

13.4 Neutralisation of IIS4 and IIIS4 charges has less effect on voltage dependence of inactivation

Figures 18 a and b illustrate the effects of charge neutralisations in segments IIS4 and IIIS4 on the inactivation curves. While CaV1.2 tolerate complete removal of all IIS4 charges, expression of functional IIIS4 mutants requires the presence of two charged residues in positions R1041+R1037 (corresponding to R6, R5 in Figure 6,).

Consequently, the starting points for estimation of the impact of IIS4 and IIIS4 were constructs with completely (IIS4) or partially neutralized (IIIS4) segments [4].

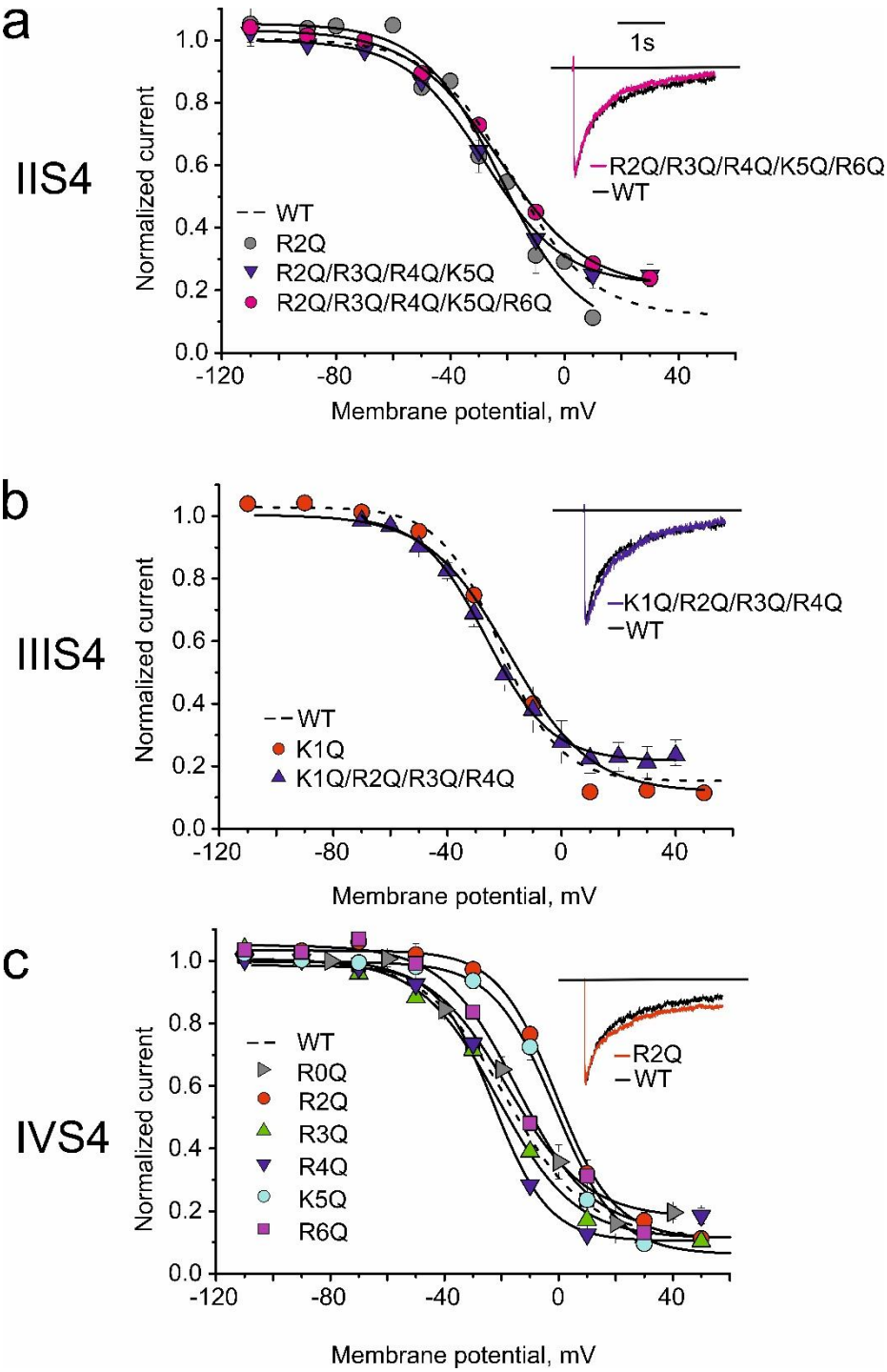


Figure 18.

Effect of charge neutralization in IIS4, IIIS4 and IVS4 on steady-state inactivation.

Steady-state inactivation (left panels) and activation (right panels) curves of WT, IIS4-IIIS4 and IVS4-mutants. Representative barium currents through WT and mutant

channels during a 3000-ms depolarization from -80 mV to the peak potential (PP) of the I-V curves are shown in corresponding insets. WT (PP: 10 mV); IIS4(R2Q/R3Q/R4Q/K5Q/R6Q) (PP: 10 mV); IIIS4(K1Q/R2Q/R3Q/R4Q) (PP: 10 mV), IVS4(R2Q) (PP: 20 mV). Figure modified from Andranovits et al. [6]

Neither neutralisation of all IIS4 charges (IIS4(R2Q/R3Q/R4Q/K5Q /R6Q)) nor partial neutralisation of IIS4 or IIIS4 (IIIS4(K1Q/R2Q/R3Q/R4Q)) shifted the midpoints ($V_{0.5,inact}$) by more than 10 mV (Figure 18 a,b) [6].

Representative currents of IIS4(R2Q/R3Q/R4Q/K5Q/R6Q), IIIS4(K1Q/R2Q/R3Q/R4Q) and currents through WT channels at the peak of the current voltage relationship illustrate inactivation kinetics identical to WT (insets in Figure 18 a, b). Similar observations were made for other IIS4 mutants or IIIS4 constructs (Figure 18a, b). Taken together, substitutions of charged residues in these segments induced only small changes in the voltage-dependence of inactivation compared to the pronounced and gradual effects observed for IS4 mutations on $V_{0.5,inact.}$ and k_{inact} (Figure 19, see Table 3, see similar small effects in activation curves in Figure 9b and c) [6].

13.5 Positional specific effects of IVS4 charge neutralisation on voltage dependence of inactivation

Combined neutralisation of two IVS4 charges prevented formation of functional channel constructs [4]. We have therefore investigated the individual contributions of each of the six IVS4 charges (Figure 8). Figure 18c illustrates the corresponding steady-state inactivation curves. Mutations IVS4(R2Q) and IVS4(K5Q) induced significant rightward shifts of inactivation curves ($\Delta V_{0.5,inact}$(IVS4(R2Q))=-0.9±1.3 mV; $\Delta V_{0.5,inact}$(IVS4(K5Q))=-5.6±1.3 mV) towards more depolarized voltages (Figure 18 c) that were accompanied by shifts of the activation curves in the same direction ($\Delta V_{0.5,act.}$(IVS4(R2Q))=15.0±0.4; $\Delta V_{0.5,\ act}$(IVS4(K5Q))=8.9±0.3 , Figure 9d, Table 3). Other mutations induced only small or negligible changes. The effects of IVS4 charge neutralisations on the slope factor of the inactivation curve are illustrated in Figure 19d [6] .

14 Discussion

The channel gating is determined by at least two distinct sub-processes: movement of VSs as well as opening and closure of S6 gates [5]. Thus, alterations of channel opening kinetics could result from one of these processes. Multiple investigations support the view that in this chain of events, the concerted pore opening is a rate-limiting stage [4].

Here, I investigate the role of segments IS4–IVS4 in gating of CaV1.2 in more detail by studying the effects of neutralization of S4 segments of different domains on inactivation, activation/deactivation kinetics and the Boltzmann distribution (steady-state activation curve).

For inactivation studies were used VS mutants, for deactivation combination of VS mutants with GAGA mutations and for activation both VS mutants alone and combination of them with GAGA mutations.

14.1 Activation is mainly determined by IS4 and to a lesser extent by S4 segments of other domains

Changes in the slope of the activation curve (Boltzmann distribution) were predominantly induced by charge neutralizations in segments IS4 (Figs. 9a and 19a). If S4 segments in CaV1.2 move not simultaneously, then the upward movement of IS4 would be rate limiting for the pore opening step. This assumption is in line with Pantazias et al [190], showing that S4 segments of different CaV1.2 domains move with different speed during activation [4].

Functional channels were formed with four out of five IS4 charges (IS4(K1Q/R2Q/R3Q/R4Q)), completely neutralized IIS4 (IIS4(R2Q/R3Q/R4Q/K5Q)), two out of six IIIS4 charges (IIIS4(K1Q/R2Q/R3Q/R4Q)) and four out of five IVS4 charges (six single point mutations) [6].

Significant effects on the slope of the activation curve observed for most IS4 constructs (except IS4(K1Q)) suggest that this segment plays a particular role in channel opening.

Only single point mutations of upper charges in domain IIS4 and IIIS4 (IIS4(R2Q) and IIIS4(IIIS4(K1Q)) and a lower charge in IVS4 (IVS4(R6Q)) affected the slope of the activation curve (Figure 10), suggesting possible involvement of these single charges in the channel opening process.

Since the R6 is laying in the lowest position of VSDIV this charge potentially may interact during the upward movement with most countercharges of S2 and S3 segments, depending on the movement of IVS4. However, to support this assumption additional experiments of counter charges neutralization are needed.

R2 charge of IVS4 may interact with aspartic acid in IVS3 segment (D1327). Interestingly, this negatively charged residue is highly conserved throughout the CaV family [1].

Costé de Bagneaux et al. [149] hypothesized that interaction between R2 and D1327 may determine the voltage dependence of activation in CaV1.2. Neutralization of the aspartic acid to the asparagine (D1327N) caused 5 mV statistically insignificant shift of activation curve to the right and significantly reduced current density [149]. This finding is in the line with my finding where neutralization of R2 in IVS4 induced the most significant shift of the activation curve (around 15 mV) among all IVS4 single point mutants.

It is hypothesized that IS4 activation occurs via sub-states, where positive charges of VSs interact sequentially with negative charges of CTC [6, 47].

The change in the slope factor may be explained by the disruption of the interaction between positive charges in the VSs and potential negative counter charges in S1, S2 and S3 segments (Figure 21). “R2”, laying in the upper position of VSDII may interact with negatively charged glutamic acid (E574). The uppermost lysine (K1) of the VSDIII lays in proximity to E950 and may interact with this residue (Figure 21).

Interestingly, all four positively charged residues of IS4 (K1, R2, R3 and R4) above the CTC can form salt-bridge interactions with aspartic and glutamic acids from the second

segment (K1 with D180, R2 with E190, R3 with E190 and E193 and R4 with E193 and R5 with E203 (see Figure 21)) [6]. This implicates, that upon depolarization, the charged residues on the IS4 segment interact sequentially with these acidic residues on S2 segments [51], [52], [222] , which supports the hypothesis that IS4 activation occurs via sub-states [6].

Individual impacts of IS4, IIS4 and IIIS4 on CaV1.2 gating become even more evident in the studied pore mutants (GAGA).

These slowly gating CaV1.2 constructs are apparently an excellent experimental platform for analyzing the effects of even single S4 charges on CaV1.2 current kinetics (Figure 11) [4].

If slow-gating GAGA mutations were used, neutralisation of S4 charges caused increase of the slope in most of GAGA+VS mutant combinations (Table2) [4]. Although, the combination A780T+IS4(K1Q/R2Q/R3Q/R4Q) displayed the most prominent change in the activation curve slope (Table 2).

14.2 Key role of IS4 in CaV1.2 inactivation

Pronounced shifts of the inactivation curve upon replacement of IS4 charges by glutamines compared to small changes in IIS4 and IIIS4 mutants highlight the principle role of IS4 in inactivation of CaV1.2 (Figs. 9 and 19). This is particular evident from Figure 19 illustrating pronounced and gradual shifts of $V_{0.5,inact}$ observed for IS4 mutations compared to small changes caused by neutralisation of individual or multiple charges in IIS4 and IIIS4 [6].

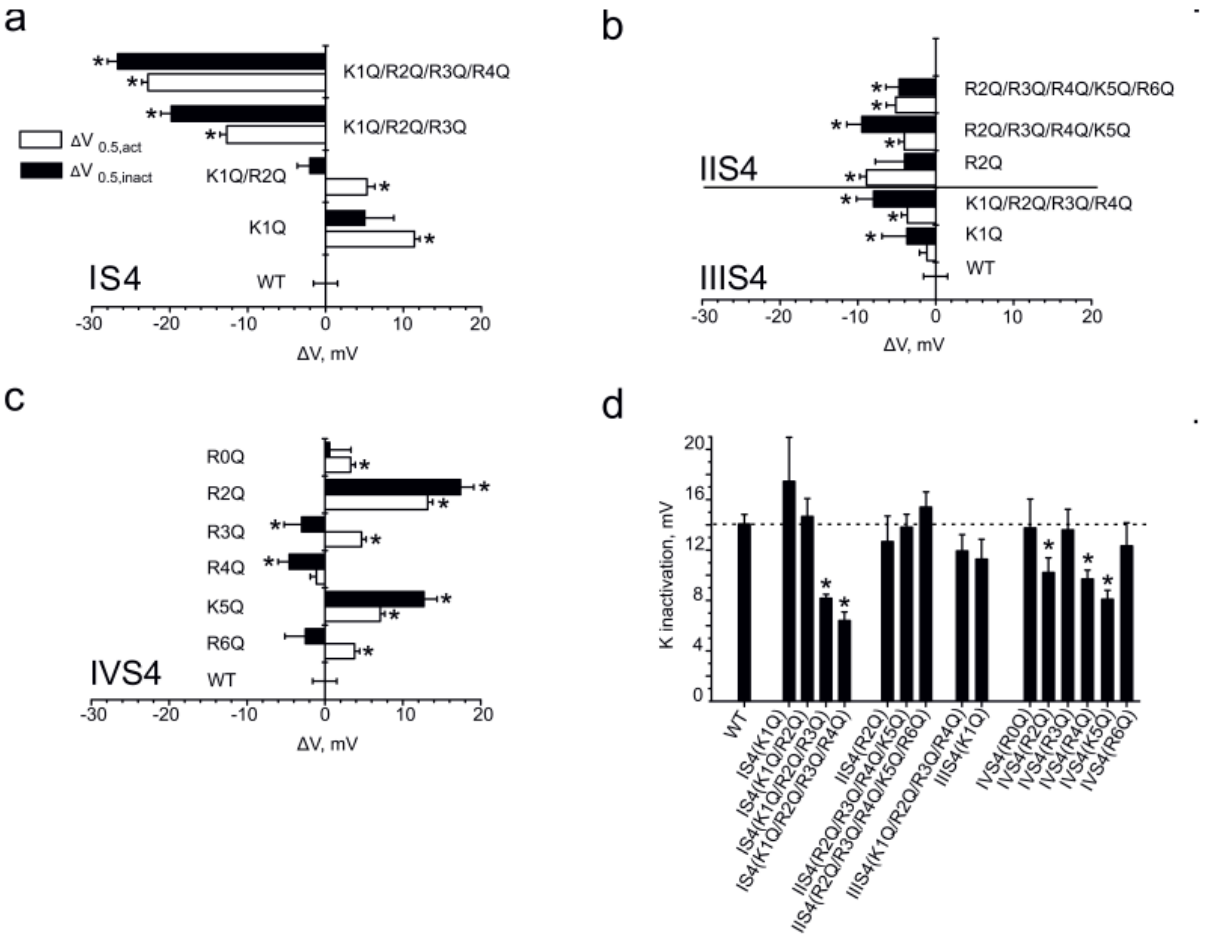


Figure 19.

Charge neutralizations in CaV1.2 segments IS4–IVS4 differently affect the position and slope of the inactivation curve. Figure from Andranovits et al. [6].

a-c Shifts of the midpoint voltages ($V_{0.5,inact}$ closed bars, $V_{0.5,act}$ open bars) of (A) IS4-, (B) IIS4- and IIIS4- and (C) IVS4-mutants compared to WT . **d** Slope factors of inactivation curves were significantly (*$p < 0.05$) decreased by charge neutralization in IS4 and IVS4. Strongest changes were observed for mutants IS4((K0Q/R1Q/R2Q) with $k_{inact.}$=8.2±0.6 mV; IS4(K1Q/R2Q/R3Q/R4Q) with $k_{inact.}$=6.2±0.7 mV; IVS4(R2Q) with $k_{inact.}$=10.2±1.2 mV; IVS4(R4Q) with $k_{inact.}$=9.7±0.7 mV and IVS4(K5Q) with $k_{inact.}$=8.1±0.7 mV. Neutralization of either single or combined charge neutralisations in IIS4 and IIIS4 had no significant effect on the slope factors of steady-state inactivation curves (Table 3).

14.3 Can charge neutralisation in IS4 enhance voltage dependence of inactivation?

The reduction of the slope factors upon charge neutralisation (Figure 19d) compared to irregular and smaller changes in other segments is a further indication of a principal

role of IS4 in inactivation (Figure 19, Table 3). Formal fitting of these curves to a simple two state Boltzmann distribution yields a paradoxical increase of the effective charge upon neutralisation of the physical charge in the VSD [6].

How can a neutralisation of IS4 charges by glutamines enhance voltage-dependence? Theoretical work of Bezanilla and Villalba-Galea [223] indicates that a simple Boltzmann fit is not applicable for estimation of the effective charge (moving charge times the fraction of the field) if S4 segments move in multiple steps via substates. In such a scenario the distribution between inactivated and available channels is more shallow than predicted by a two state Boltzmann function and the slope of the curve is maximal when there are only two states [6, 223].

It is thus tempting to speculate that IS4 in WT channels moves via sub-states that are transiently stabilised by interactions of arginines (and lysines) with surrounding residues [224].

Replacing these charged residues by neutral glutamines would consequently disrupt these interactions, thereby reducing the number of IS4 substates and decreasing the slope factor of the inactivation curve. Such a hypothesis is also supported by the acceleration of inactivation observed upon stepwise charge IS4 neutralisation (Figure 16d). Hence, removal of IS4 interactions is expected to ease IS4 movements towards an “inactivating” up position [6].

The cryo-electron microscopy structure of the CaV1.1channel and the deduced atomic model provide a good template for interpretations of interactions of voltage sensors with surrounding residues [206]. Positive charges of S4-segments are stabilized in different conformations by polar and negatively charged residues located in the S1–S3 helices. [38, 39, 60, 213, 225]. A “gating charge transfer center” (CTC) that has a phenylalanine in S2 and negatively charged residues in S2 and S3 has been identified in voltage-gated potassium and sodium channels [86, 226, 227]. H-bonds transiently stabilize charged S4 residues in proximity to the CTC [227, 228, 6]. Interestingly, in the upstate, IS4 can potentially form up to 5 salt bridges above the CTC (7 in total) which distinguishes this VSD from domains in segments II –IV (Figures 20,21) [6].

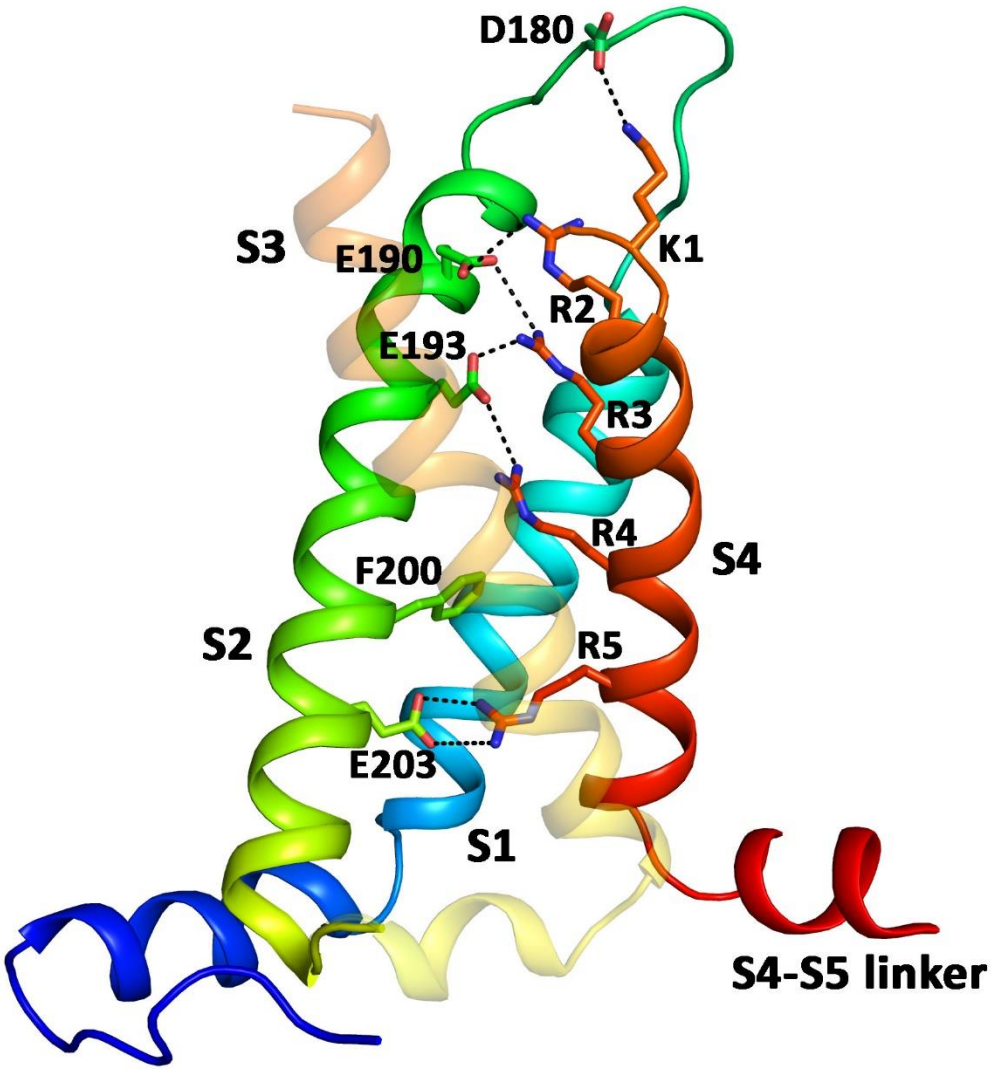


Figure 20.

Potential interactions of the S4 charged residues in VSD I. S1, S2, S3 and S4 presented as cartoon in blue, green, yellow and red, respectively. Charged residues represented as sticks. Charge interaction possibilities are highlighted as black dash lines. For clarity reasons, the S3 is slightly transparent. Figure from “Supplemental materials” Andranovits et al. [6].

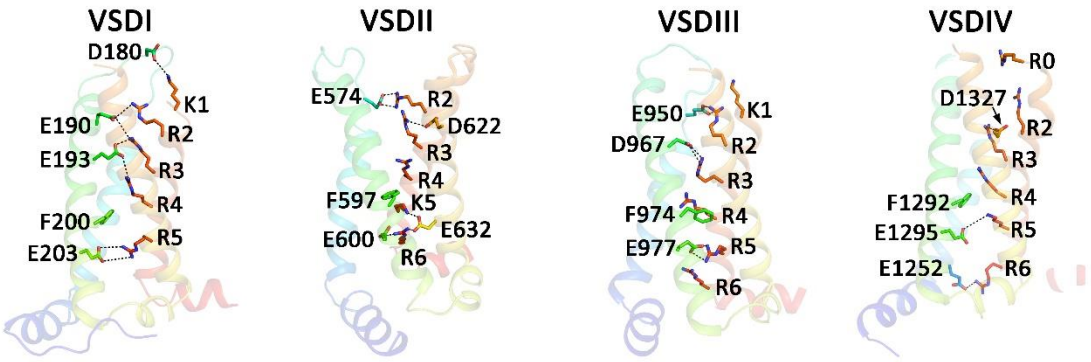


Figure 21.

VSDI-IV interactions of the positively charged S4 residues. Cartoon representation of the S1-S4 helices. Charged residues that can interact are shown as sticks. Interaction possibilities are shown as dashed lines. Maximum distance for interactions was 4Å. Figure modified from “Supplemental materials” Andranovits et al. [6].

14.4 Role of IVS4 in inactivation gating

In order to get insights into the role of IVS4 in CaV1.2 inactivation we neutralized all six charges individually. Two mutations shifted voltage-dependence of channel gating (R2Q: $\Delta V_{0.5,inact}$= -0.9±1.3 mV; K5Q: $\Delta V_{0.5,inact}$= -5.6±1.3 mV) significantly towards more positive voltages. The gating behaviour of other mutants was not significantly different from WT. The rightward shifts of activation and inactivation curves caused by IVS4(R2Q) and IVS4(K5Q) suggest that these charged residues interact with surrounding amino acids that stabilise the voltage sensor in an open activated position or destabilise its conformation in the resting state, or both (Figure 21) [6].

Modelling of the side chain salt-bridge interactions in VSD IV shows only one aspartic acid above the CTC, D1327, which can potentially interact with the positively charged IVS4 residues. In the cryo-EM structure D1327 interacts with R3; however, during the upward movement of the voltage sensor, interactions with R0 and R2 are conceivable (Figure 21) [6].

14.5 Activation and inactivation of CaV1.2 are linked via segment IS4

There is a good evidence that activation of voltage gated ion channels is associated with conformational changes at the inner helix bundle enabling dissociation of S6

segments and pore opening [41]. Voltage-dependent inactivation is likely to involve structural changes at the outer channel mouth at the selectivity filter [214, 229-232]. Evidence for a close link between the activation and inactivation gates in CaV1.2 comes from multiple observations that perturbations of the activation gate (inner helix bundle) usually affect voltage gated inactivation . Thus, significant correlations between the shifts of the activation and inactivation curves caused by mutations on segments IS6 – IVS6 (Figure 22) suggest that conformational changes at the inner helical bundle are coupled to the inactivation gate [1-3; 6].

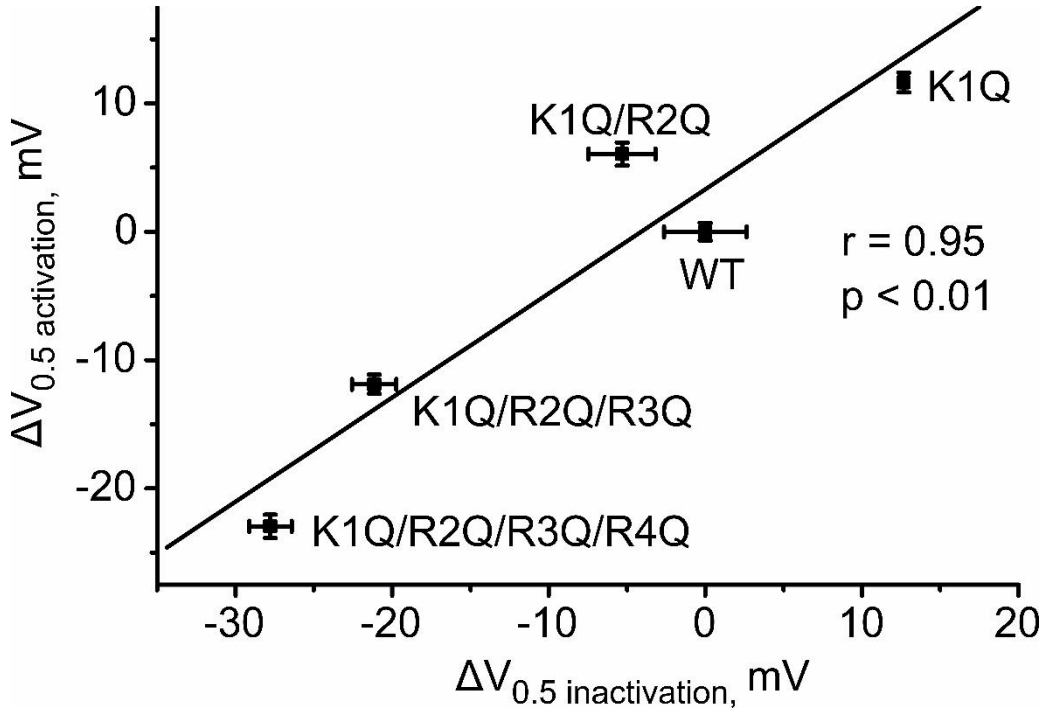


Figure 22.

Correlation between potentials of half-maximal activation ($V_{0.5,act}$) and half-maximal inactivation ($V_{0.5,inact}$) of IS4 mutants (Table 3). Linear regression analysis (solid line) yielded a statistically significant linear correlation ($p<0.01$) with a correlation coefficient of 0.95. Figure from Andranovits et al. [6].

15 Summary

In the present studies I investigated the influence of charge neutralization in segments IS4-IVS4 on CaV1.2 gating.

A principal finding of my study was that IS4 plays a key role in both, voltage-dependent inactivation and activation. Impairing IS4 function by charge neutralization (Figure 8) had the largest and regular (charge dependent) effects on voltage-dependent inactivation compared to no or less impact of equivalent charge neutralizations in segments IIS4 and IIIS4 [5]. Furthermore, stepwise neutralization of IS4 charges induced a parallel and gradual reduction of the slope factor of the inactivation curve (Figure 19 d) [6].

A gradual reduction of the slope factor of the inactivation curve on stepwise neutralization of IS4 charges is shown in Figure 19 d. Apparent enhancement of inactivation caused by IS4 neutralization is also evident from the accelerated time course of current decay (Figure 16b). This steeper voltage dependence can be understood assuming that IS4 moves through substates that are stabilized by interactions of IS4 charges with surrounding residues (Figure 20). In this scenario, neutralization of these charges reduces the number of interactions (e.g., salt bridges) and correspondingly the number of sub-states that IS4 can occupy (Figure20) between full activation and inactivation . The role of IS4 substates and there structural basis (corresponding interactions with neighboring segments) have yet to be clarified [6].

Movement of IS4 is rate-limiting for activation. Single point mutations that affect activation were found also in S4 segments of other domains (Figure 10, Figure 19, Table 3), but these changes in the gating were neither large nor consistent, as in the case of IS4 (Figure 19) [6].

Combination of slowly-gating GAGA mutants with neutralization of VSs confirmed this finding, highlighting the principle role of IS4 in activation [4].

Furthermore, studies with the slowly gating pore mutants (GAGA) suggested that IS4–IIIS4 all contribute to stabilisation of the open channel conformation . This is evident from the acceleration of the channel deactivation caused by charge neutralisation of the different S4 segments (Figure15 b) [4].

Shifts in the voltage dependence of inactivation curves induced by IS4 neutralizations significantly correlated with shifts of the voltage dependence of channel activation ($r = 0.95$, $p < 0.01$) indicating that IS4 movement is not only rate limiting for activation but also initiates inactivation (Figure 22) [6].

The role of IVS4 in gating remains unclear and requires additional studies.

16 Acknowledgements

I thank my academic and scientific supervisor at the University of Vienna Prof. Steffen Hering for the opportunity to perform this work in frame of the MolTag PhD program. This would not have been done without his immediate help, advice and directions.

I am deeply indebted to FWF Vienna for the financial support and to University of Vienna for providing me with superb technical facilities and a friendly working atmosphere. I am grateful to all my colleagues, who could support me during performance of my experiments.

A very special thank goes to Dr.Stanislav Beyl for introducing me to the practical part of the electrophysiology, for training me at the first steps and answering my questions in the theory of biophysics.

The mutations that I have used in my biophysical studies were created by Dr. Annette Hohaus and I would like to thank her for this important input.

I would like to extend my warmest thanks to Dr. Igor Baburin for his willingness to help me both in scientific and not-work related problems and for our deep scientific discussions during our lunch.

I also want to thank my colleagues from the MolTag doctoral program for the great time during the nice social events we had together.

I want to give my special thanks our secretary Susanne Menschik-Zunzer for her kindness to help me with documents and paperwork and always sharing positive attitude.

Last but not least I want to thank my parents Viatcheslav and Natalja for making this all possible and my brother Bogdan for his support!

17 References

1. Depil, K., et al., *Timothy mutation disrupts the link between activation and inactivation in Ca(V)1.2 protein.* J Biol Chem, 2011. **286**(36): p. 31557-64.
2. Hohaus, A., et al., *Structural determinants of L-type channel activation in segment IIS6 revealed by a retinal disorder.* J Biol Chem, 2005. **280**(46): p. 38471-7.
3. Kudrnac, M., et al., *Coupled and independent contributions of residues in IS6 and IIS6 to activation gating of CaV1.2.* J Biol Chem, 2009. **284**(18): p. 12276-84.
4. Beyl, S., et al., *Upward movement of IS4 and IIIS4 is a rate-limiting stage in CaV1.2 activation.* Pflugers Arch, 2016. **468**(11-12): p. 1895-1907.
5. Hering, S., et al., *Calcium channel gating.* Pflugers Arch, 2018. **470**(9): p. 1291-1309.
6. Andranovits, S., et al., *Key role of segment IS4 in CaV1.2 inactivation: link between activation and inactivation.* Pflugers Arch, 2017. **469**(11): p. 1485-1493.
7. Hemara-Wahanui, A., et al., *A CACNA1F mutation identified in an X-linked retinal disorder shifts the voltage dependence of CaV1.4 channel activation.* Proc Natl Acad Sci U S A, 2005. **102**(21): p. 7553-8.
8. Simms, B.A., I.A. Souza, and G.W. Zamponi, *Effect of the Brugada syndrome mutation A39V on calmodulin regulation of CaV1.2 channels.* Mol Brain, 2014. **7**: p. 34.
9. Barrett, C.F. and R.W. Tsien, *The Timothy syndrome mutation differentially affects voltage- and calcium-dependent inactivation of CaV1.2 L-type calcium channels.* Proc Natl Acad Sci U S A, 2008. **105**(6): p. 2157-62.
10. Nanou, E. and W.A. Catterall, *Calcium Channels, Synaptic Plasticity, and Neuropsychiatric Disease.* Neuron, 2018. **98**(3): p. 466-481.
11. Bezanilla, F., *The voltage sensor in voltage-dependent ion channels.* Physiol Rev, 2000. **80**(2): p. 555-92.
12. Hille, B., *Ionic channels: molecular pores of excitable membranes.* Harvey Lect, 1986. **82**: p. 47-69.
13. Ugarte, G., F. Perez, and R. Latorre, *How do calcium channels transport calcium ions?* Biol Res, 1998. **31**(1): p. 17-32.
14. Catterall, W.A., *Voltage-gated calcium channels.* Cold Spring Harb Perspect Biol, 2011. **3**(8): p. a003947.
15. Alexander, S.P., et al., *THE CONCISE GUIDE TO PHARMACOLOGY 2017/18: Overview.* Br J Pharmacol, 2017. **174 Suppl 1**: p. S1-S16.
16. Carbone, E. and H.D. Lux, *A low voltage-activated, fully inactivating Ca channel in vertebrate sensory neurones.* Nature, 1984. **310**(5977): p. 501-2.
17. Nilius, B., et al., *A novel type of cardiac calcium channel in ventricular cells.* Nature, 1985. **316**(6027): p. 443-6.
18. Perez-Reyes, E., *Molecular physiology of low-voltage-activated t-type calcium channels.* Physiol Rev, 2003. **83**(1): p. 117-61.
19. Perez-Reyes, E., et al., *Molecular characterization of a neuronal low-voltage-activated T-type calcium channel.* Nature, 1998. **391**(6670): p. 896-900.
20. Perez-Reyes, E. and J.H. Lee, *Ins and outs of T-channel structure function.* Pflugers Arch, 2014. **466**(4): p. 627-33.
21. Zamponi, G.W., *A Crash Course in Calcium Channels.* ACS Chem Neurosci, 2017. **8**(12): p. 2583-2585.

22. Dolphin, A.C., *A short history of voltage-gated calcium channels.* Br J Pharmacol, 2006. **147 Suppl 1**: p. S56-62.
23. Catterall, W.A., et al., *International Union of Pharmacology. XLVIII. Nomenclature and structure-function relationships of voltage-gated calcium channels.* Pharmacol Rev, 2005. **57**(4): p. 411-25.
24. Hofmann, F., et al., *L-type CaV1.2 calcium channels: from in vitro findings to in vivo function.* Physiol Rev, 2014. **94**(1): p. 303-26.
25. Striessnig, J., et al., *L-type Ca(2+) channels in heart and brain.* Wiley Interdiscip Rev Membr Transp Signal, 2014. **3**(2): p. 15-38.
26. Karaki, H., et al., *Calcium movements, distribution, and functions in smooth muscle.* Pharmacol Rev, 1997. **49**(2): p. 157-230.
27. T.Feng, S.K., K.Barakat, *L-Type Calcium Channels: Structure and Functions.* IntechOpen, 2018. **7**: p. 127-148.
28. Striessnig, J., H.J. Bolz, and A. Koschak, *Channelopathies in CaV1.1, CaV1.3, and CaV1.4 voltage-gated L-type Ca^{2+} channels.* Pflugers Arch, 2010. **460**(2): p. 361-74.
29. Terwindt, G.M., et al., *Migraine, ataxia and epilepsy: a challenging spectrum of genetically determined calcium channelopathies. Dutch Migraine Genetics Research Group.* Eur J Hum Genet, 1998. **6**(4): p. 297-307.
30. Carrera, P., et al., *Familial hemiplegic migraine: a ion channel disorder.* Brain Res Bull, 2001. **56**(3-4): p. 239-41.
31. Jurkat-Rott, K., H. Lerche, and F. Lehmann-Horn, *Skeletal muscle channelopathies.* J Neurol, 2002. **249**(11): p. 1493-502.
32. Becker, C., S.S. Jick, and C.R. Meier, *Use of antihypertensives and the risk of Parkinson disease.* Neurology, 2008. **70**(16 Pt 2): p. 1438-44.
33. Ritz, B., et al., *L-type calcium channel blockers and Parkinson disease in Denmark.* Ann Neurol, 2010. **67**(5): p. 600-6.
34. Baig, S.M., et al., *Loss of Ca(v)1.3 (CACNA1D) function in a human channelopathy with bradycardia and congenital deafness.* Nat Neurosci, 2011. **14**(1): p. 77-84.
35. Zhang, Z., et al., *Functional Roles of Ca(v)1.3 (alpha(1D)) calcium channel in sinoatrial nodes: insight gained using gene-targeted null mutant mice.* Circ Res, 2002. **90**(9): p. 981-7.
36. Scholl, U.I., et al., *Somatic and germline CACNA1D calcium channel mutations in aldosterone-producing adenomas and primary aldosteronism.* Nat Genet, 2013. **45**(9): p. 1050-4.
37. Stockner, T. and A. Koschak, *What can naturally occurring mutations tell us about Ca(v)1.x channel function?* Biochim Biophys Acta, 2013. **1828**(7): p. 1598-607.
38. Wu, J., et al., *Structure of the voltage-gated calcium channel Ca(v)1.1 at 3.6 A resolution.* Nature, 2016. **537**(7619): p. 191-196.
39. Wu, J., et al., *Structure of the voltage-gated calcium channel CaV1.1 complex.* Science, 2015. **350**(6267): p. aad2395.
40. Arikkath, J. and K.P. Campbell, *Auxiliary subunits: essential components of the voltage-gated calcium channel complex.* Curr Opin Neurobiol, 2003. **13**(3): p. 298-307.
41. Catterall, W.A., *Structure and regulation of voltage-gated Ca^{2+} channels.* Annu Rev Cell Dev Biol, 2000. **16**: p. 521-55.
42. Hering, S., *beta-Subunits: fine tuning of $Ca^{(2+)}$ channel block.* Trends Pharmacol Sci, 2002. **23**(11): p. 509-13.

43. B.S. Barker1, G.T.Y., C.H. Soubrane2, G.J. Stephens3, E.B. Stevens2, M.K. Patel1, *Chapter 2 - Ion Channels.* Conn's Translational Neuroscience, 2017: p. 11-43.
44. Hille, B., *Ion channels of excitable membranes*. 3rd ed. 2001, Sunderland, Mass.: Sinauer. xviii, 814 p.
45. Van Petegem, F. and D.L. Minor, Jr., *The structural biology of voltage-gated calcium channel function and regulation.* Biochem Soc Trans, 2006. **34**(Pt 5): p. 887-93.
46. Catterall, W.A., *Ion channel voltage sensors: structure, function, and pathophysiology.* Neuron, 2010. **67**(6): p. 915-28.
47. Tuluc, P., et al., *Molecular Interactions in the Voltage Sensor Controlling Gating Properties of CaV Calcium Channels.* Structure, 2016. **24**(2): p. 261-71.
48. Payandeh, J., et al., *Crystal structure of a voltage-gated sodium channel in two potentially inactivated states.* Nature, 2012. **486**(7401): p. 135-9.
49. Payandeh, J., et al., *The crystal structure of a voltage-gated sodium channel.* Nature, 2011. **475**(7356): p. 353-8.
50. Tao, X., et al., *A gating charge transfer center in voltage sensors.* Science, 2010. **328**(5974): p. 67-73.
51. DeCaen, P.G., et al., *Disulfide locking a sodium channel voltage sensor reveals ion pair formation during activation.* Proc Natl Acad Sci U S A, 2008. **105**(39): p. 15142-7.
52. DeCaen, P.G., et al., *Sequential formation of ion pairs during activation of a sodium channel voltage sensor.* Proc Natl Acad Sci U S A, 2009. **106**(52): p. 22498-503.
53. Cheng, Y.M., et al., *Functional interactions of voltage sensor charges with an S2 hydrophobic plug in hERG channels.* J Gen Physiol, 2013. **142**(3): p. 289-303.
54. Lin, M.C., et al., *R1 in the Shaker S4 occupies the gating charge transfer center in the resting state.* J Gen Physiol, 2011. **138**(2): p. 155-63.
55. Yarov-Yarovoy, V., et al., *Structural basis for gating charge movement in the voltage sensor of a sodium channel.* Proc Natl Acad Sci U S A, 2012. **109**(2): p. E93-102.
56. Ellinor, P.T., et al., *Ca2+ channel selectivity at a single locus for high-affinity Ca2+ interactions.* Neuron, 1995. **15**(5): p. 1121-32.
57. Yang, J., et al., *Molecular determinants of Ca2+ selectivity and ion permeation in L-type Ca2+ channels.* Nature, 1993. **366**(6451): p. 158-61.
58. Cataldi, M., E. Perez-Reyes, and R.W. Tsien, *Differences in apparent pore sizes of low and high voltage-activated Ca2+ channels.* J Biol Chem, 2002. **277**(48): p. 45969-76.
59. Hering, S., et al., *Ca2+ channel block and inactivation: common molecular determinants.* Trends Pharmacol Sci, 1998. **19**(11): p. 439-43.
60. Striessnig, J., N.J. Ortner, and A. Pinggera, *Pharmacology of L-type Calcium Channels: Novel Drugs for Old Targets?* Curr Mol Pharmacol, 2015. **8**(2): p. 110-22.
61. Benmocha Guggenheimer, A., et al., *Interactions between N and C termini of alpha1C subunit regulate inactivation of CaV1.2 L-type $Ca^{(2+)}$ channel.* Channels (Austin), 2016. **10**(1): p. 55-68.

62. Minor, D.L., Jr. and F. Findeisen, *Progress in the structural understanding of voltage-gated calcium channel (CaV) function and modulation.* Channels (Austin), 2010. **4**(6): p. 459-74.
63. Snutch, T.P., *Voltage-Gated Calcium Channels.* Encyclopedia of Neuroscience, 2009. **10**: p. 427-441.
64. Takahashi, S.X., J. Miriyala, and H.M. Colecraft, *Membrane-associated guanylate kinase-like properties of beta-subunits required for modulation of voltage-dependent Ca2+ channels.* Proc Natl Acad Sci U S A, 2004. **101**(18): p. 7193-8.
65. Jones, L.P., S.K. Wei, and D.T. Yue, *Mechanism of auxiliary subunit modulation of neuronal alpha1E calcium channels.* J Gen Physiol, 1998. **112**(2): p. 125-43.
66. Josephson, I.R. and G. Varadi, *The beta subunit increases Ca2+ currents and gating charge movements of human cardiac L-type Ca2+ channels.* Biophys J, 1996. **70**(3): p. 1285-93.
67. Beguin, P., et al., *Regulation of Ca2+ channel expression at the cell surface by the small G-protein kir/Gem.* Nature, 2001. **411**(6838): p. 701-6.
68. Bichet, D., et al., *The I-II loop of the Ca2+ channel alpha1 subunit contains an endoplasmic reticulum retention signal antagonized by the beta subunit.* Neuron, 2000. **25**(1): p. 177-90.
69. Costantin, J., et al., *Facilitation by the beta2a subunit of pore openings in cardiac Ca2+ channels.* J Physiol, 1998. **507 (Pt 1)**: p. 93-103.
70. Singer, D., et al., *The roles of the subunits in the function of the calcium channel.* Science, 1991. **253**(5027): p. 1553-7.
71. Perez-Reyes, E., et al., *Cloning and expression of a cardiac/brain beta subunit of the L-type calcium channel.* J Biol Chem, 1992. **267**(3): p. 1792-7.
72. Colecraft, H.M., et al., *Novel functional properties of $Ca^{(2+)}$ channel beta subunits revealed by their expression in adult rat heart cells.* J Physiol, 2002. **541**(Pt 2): p. 435-52.
73. Hullin, R., et al., *Cardiac L-type calcium channel beta-subunits expressed in human heart have differential effects on single channel characteristics.* J Biol Chem, 2003. **278**(24): p. 21623-30.
74. Altier, C., et al., *The CaVbeta subunit prevents RFP2-mediated ubiquitination and proteasomal degradation of L-type channels.* Nat Neurosci, 2011. **14**(2): p. 173-80.
75. Waithe, D., et al., *Beta-subunits promote the expression of Ca(V)2.2 channels by reducing their proteasomal degradation.* J Biol Chem, 2011. **286**(11): p. 9598-611.
76. Dolphin, A.C., *Voltage-gated calcium channels and their auxiliary subunits: physiology and pathophysiology and pharmacology.* J Physiol, 2016. **594**(19): p. 5369-90.
77. Gregg, R.G., et al., *Absence of the beta subunit (cchb1) of the skeletal muscle dihydropyridine receptor alters expression of the alpha 1 subunit and eliminates excitation-contraction coupling.* Proc Natl Acad Sci U S A, 1996. **93**(24): p. 13961-6.
78. Ball, S.L., et al., *Role of the beta(2) subunit of voltage-dependent calcium channels in the retinal outer plexiform layer.* Invest Ophthalmol Vis Sci, 2002. **43**(5): p. 1595-603.

79. Stotz, S.C. and G.W. Zamponi, *Structural determinants of fast inactivation of high voltage-activated Ca$^{(2+)}$ channels.* Trends Neurosci, 2001. **24**(3): p. 176-81.
80. Takahashi, M., et al., *Subunit structure of dihydropyridine-sensitive calcium channels from skeletal muscle.* Proc Natl Acad Sci U S A, 1987. **84**(15): p. 5478-82.
81. Castellano, A., et al., *Cloning and expression of a neuronal calcium channel beta subunit.* J Biol Chem, 1993. **268**(17): p. 12359-66.
82. Hullin, R., et al., *Calcium channel beta subunit heterogeneity: functional expression of cloned cDNA from heart, aorta and brain.* EMBO J, 1992. **11**(3): p. 885-90.
83. Takahashi, S.X., et al., *A CaVbeta SH3/guanylate kinase domain interaction regulates multiple properties of voltage-gated Ca2+ channels.* J Gen Physiol, 2005. **126**(4): p. 365-77.
84. Hanlon, M.R., et al., *Modelling of a voltage-dependent Ca2+ channel beta subunit as a basis for understanding its functional properties.* FEBS Lett, 1999. **445**(2-3): p. 366-70.
85. Dolphin, A.C., *Calcium channel auxiliary alpha2delta and beta subunits: trafficking and one step beyond.* Nat Rev Neurosci, 2012. **13**(8): p. 542-55.
86. Zamponi, G.W., et al., *The Physiology, Pathology, and Pharmacology of Voltage-Gated Calcium Channels and Their Future Therapeutic Potential.* Pharmacol Rev, 2015. **67**(4): p. 821-70.
87. Sekiguchi, F., M. Tsubota, and A. Kawabata, *Involvement of Voltage-Gated Calcium Channels in Inflammation and Inflammatory Pain.* Biol Pharm Bull, 2018. **41**(8): p. 1127-1134.
88. Felix, R., *Voltage-dependent Ca2+ channel alpha2delta auxiliary subunit: structure, function and regulation.* Receptors Channels, 1999. **6**(5): p. 351-62.
89. Davies, A., et al., *Functional biology of the alpha(2)delta subunits of voltage-gated calcium channels.* Trends Pharmacol Sci, 2007. **28**(5): p. 220-8.
90. Jay, S.D., et al., *Structural characterization of the dihydropyridine-sensitive calcium channel alpha 2-subunit and the associated delta peptides.* J Biol Chem, 1991. **266**(5): p. 3287-93.
91. De Jongh, K.S., C. Warner, and W.A. Catterall, *Subunits of purified calcium channels. Alpha 2 and delta are encoded by the same gene.* J Biol Chem, 1990. **265**(25): p. 14738-41.
92. Calderon-Rivera, A., et al., *Identification of a disulfide bridge essential for structure and function of the voltage-gated Ca(2+) channel alpha(2)delta-1 auxiliary subunit.* Cell Calcium, 2012. **51**(1): p. 22-30.
93. Canti, C., et al., *The metal-ion-dependent adhesion site in the Von Willebrand factor-A domain of alpha2delta subunits is key to trafficking voltage-gated Ca2+ channels.* Proc Natl Acad Sci U S A, 2005. **102**(32): p. 11230-5.
94. Bhattacharya, A.A., et al., *Crystal structure of the A domain from complement factor B reveals an integrin-like open conformation.* Structure, 2004. **12**(3): p. 371-8.
95. Hoppa, M.B., et al., *alpha2delta expression sets presynaptic calcium channel abundance and release probability.* Nature, 2012. **486**(7401): p. 122-5.
96. Gurnett, C.A., M. De Waard, and K.P. Campbell, *Dual function of the voltage-dependent Ca2+ channel alpha 2 delta subunit in current stimulation and subunit interaction.* Neuron, 1996. **16**(2): p. 431-40.

97. Felix, R., et al., *Dissection of functional domains of the voltage-dependent Ca2+ channel alpha2delta subunit.* J Neurosci, 1997. **17**(18): p. 6884-91.
98. Klugbauer, N., et al., *Molecular diversity of the calcium channel alpha2delta subunit.* J Neurosci, 1999. **19**(2): p. 684-91.
99. Bangalore, R., et al., *Influence of L-type Ca channel alpha 2/delta-subunit on ionic and gating current in transiently transfected HEK 293 cells.* Am J Physiol, 1996. **270**(5 Pt 2): p. H1521-8.
100. Shirokov, R., et al., *Inactivation of gating currents of L-type calcium channels. Specific role of the alpha 2 delta subunit.* J Gen Physiol, 1998. **111**(6): p. 807-23.
101. Shistik, E., et al., *Ca2+ current enhancement by alpha 2/delta and beta subunits in Xenopus oocytes: contribution of changes in channel gating and alpha 1 protein level.* J Physiol, 1995. **489 (Pt 1)**: p. 55-62.
102. Welling, A., et al., *Stable co-expression of calcium channel alpha 1, beta and alpha 2/delta subunits in a somatic cell line.* J Physiol, 1993. **471**: p. 749-65.
103. Hobom, M., et al., *Neuronal distribution and functional characterization of the calcium channel alpha2delta-2 subunit.* Eur J Neurosci, 2000. **12**(4): p. 1217-26.
104. Wakamori, M., G. Mikala, and Y. Mori, *Auxiliary subunits operate as a molecular switch in determining gating behaviour of the unitary N-type Ca2+ channel current in Xenopus oocytes.* J Physiol, 1999. **517 (Pt 3)**: p. 659-72.
105. Fuller-Bicer, G.A., et al., *Targeted disruption of the voltage-dependent calcium channel alpha2/delta-1-subunit.* Am J Physiol Heart Circ Physiol, 2009. **297**(1): p. H117-24.
106. Barclay, J., et al., *Ducky mouse phenotype of epilepsy and ataxia is associated with mutations in the Cacna2d2 gene and decreased calcium channel current in cerebellar Purkinje cells.* J Neurosci, 2001. **21**(16): p. 6095-104.
107. Brodbeck, J., et al., *The ducky mutation in Cacna2d2 results in altered Purkinje cell morphology and is associated with the expression of a truncated alpha 2 delta-2 protein with abnormal function.* J Biol Chem, 2002. **277**(10): p. 7684-93.
108. Dolphin, A.C., *Voltage-gated calcium channel alpha 2delta subunits: an assessment of proposed novel roles.* F1000Res, 2018. **7**.
109. Jay, S.D., et al., *Primary structure of the gamma subunit of the DHP-sensitive calcium channel from skeletal muscle.* Science, 1990. **248**(4954): p. 490-2.
110. Black, J.L., 3rd, *The voltage-gated calcium channel gamma subunits: a review of the literature.* J Bioenerg Biomembr, 2003. **35**(6): p. 649-60.
111. Glossmann, H., et al., *Purified L-type calcium channels: only one single polypeptide (alpha 1-subunit) carries the drug receptor domains and is regulated by protein kinases.* Biomed Biochim Acta, 1987. **46**(8-9): p. S351-6.
112. Letts, V.A., et al., *The mouse stargazer gene encodes a neuronal Ca2+-channel gamma subunit.* Nat Genet, 1998. **19**(4): p. 340-7.
113. Tseng, T.T., et al., *Calcium channel auxiliary subunits.* J Mol Microbiol Biotechnol, 2006. **11**(6): p. 326-44.
114. Moss, F.J., et al., *The novel product of a five-exon stargazin-related gene abolishes Ca(V)2.2 calcium channel expression.* EMBO J, 2002. **21**(7): p. 1514-23.

115. Muller, C.S., et al., *Quantitative proteomics of the CaV2 channel nano-environments in the mammalian brain.* Proc Natl Acad Sci U S A, 2010. **107**(34): p. 14950-7.
116. Walsh, C.P., et al., *Labelling of the 3D structure of the cardiac L-type voltage-gated calcium channel.* Channels (Austin), 2009. **3**(6): p. 387-92.
117. Tomita, S., et al., *Functional studies and distribution define a family of transmembrane AMPA receptor regulatory proteins.* J Cell Biol, 2003. **161**(4): p. 805-16.
118. Lipscombe, D., A. Andrade, and S.E. Allen, *Alternative splicing: functional diversity among voltage-gated calcium channels and behavioral consequences.* Biochim Biophys Acta, 2013. **1828**(7): p. 1522-9.
119. Hagiwara, S., S. Ozawa, and O. Sand, *Voltage clamp analysis of two inward current mechanisms in the egg cell membrane of a starfish.* J Gen Physiol, 1975. **65**(5): p. 617-44.
120. Llinas, R. and Y. Yarom, *Electrophysiology of mammalian inferior olivary neurones in vitro. Different types of voltage-dependent ionic conductances.* J Physiol, 1981. **315**: p. 549-67.
121. Reuter, H., *Calcium channel modulation by neurotransmitters, enzymes and drugs.* Nature, 1983. **301**(5901): p. 569-74.
122. Tsien, R.W., et al., *Multiple types of neuronal calcium channels and their selective modulation.* Trends Neurosci, 1988. **11**(10): p. 431-8.
123. Fedulova, S.A., P.G. Kostyuk, and N.S. Veselovsky, *Two types of calcium channels in the somatic membrane of new-born rat dorsal root ganglion neurones.* J Physiol, 1985. **359**: p. 431-46.
124. Nowycky, M.C., A.P. Fox, and R.W. Tsien, *Three types of neuronal calcium channel with different calcium agonist sensitivity.* Nature, 1985. **316**(6027): p. 440-3.
125. Park, J. and Z.D. Luo, *Calcium channel functions in pain processing.* Channels (Austin), 2010. **4**(6): p. 510-7.
126. Dolphin, A.C., *Voltage-gated calcium channels: their discovery, function and importance as drug targets.* Brain Neurosci Adv, 2018. **2**.
127. Olivera, B.M., et al., *Calcium channel diversity and neurotransmitter release: the omega-conotoxins and omega-agatoxins.* Annu Rev Biochem, 1994. **63**: p. 823-67.
128. Boland, L.M., J.A. Morrill, and B.P. Bean, *omega-Conotoxin block of N-type calcium channels in frog and rat sympathetic neurons.* J Neurosci, 1994. **14**(8): p. 5011-27.
129. Plummer, M.R., D.E. Logothetis, and P. Hess, *Elementary properties and pharmacological sensitivities of calcium channels in mammalian peripheral neurons.* Neuron, 1989. **2**(5): p. 1453-63.
130. Hirning, L.D., et al., *Dominant role of N-type Ca2+ channels in evoked release of norepinephrine from sympathetic neurons.* Science, 1988. **239**(4835): p. 57-61.
131. Mintz, I.M., et al., *P-type calcium channels blocked by the spider toxin omega-Aga-IVA.* Nature, 1992. **355**(6363): p. 827-9.
132. Randall, A. and R.W. Tsien, *Pharmacological dissection of multiple types of Ca2+ channel currents in rat cerebellar granule neurons.* J Neurosci, 1995. **15**(4): p. 2995-3012.

133. Soong, T.W., et al., *Structure and functional expression of a member of the low voltage-activated calcium channel family.* Science, 1993. **260**(5111): p. 1133-6.
134. Curtis, B.M. and W.A. Catterall, *Purification of the calcium antagonist receptor of the voltage-sensitive calcium channel from skeletal muscle transverse tubules.* Biochemistry, 1984. **23**(10): p. 2113-8.
135. Tanabe, T., et al., *Primary structure of the receptor for calcium channel blockers from skeletal muscle.* Nature, 1987. **328**(6128): p. 313-8.
136. Mikami, A., et al., *Primary structure and functional expression of the cardiac dihydropyridine-sensitive calcium channel.* Nature, 1989. **340**(6230): p. 230-3.
137. Biel, M., et al., *Primary structure and functional expression of a high voltage activated calcium channel from rabbit lung.* FEBS Lett, 1990. **269**(2): p. 409-12.
138. Seino, S., et al., *Cloning of the alpha 1 subunit of a voltage-dependent calcium channel expressed in pancreatic beta cells.* Proc Natl Acad Sci U S A, 1992. **89**(2): p. 584-8.
139. Williams, M.E., et al., *Structure and functional expression of alpha 1, alpha 2, and beta subunits of a novel human neuronal calcium channel subtype.* Neuron, 1992. **8**(1): p. 71-84.
140. Strom, T.M., et al., *An L-type calcium-channel gene mutated in incomplete X-linked congenital stationary night blindness.* Nat Genet, 1998. **19**(3): p. 260-3.
141. Bech-Hansen, N.T., et al., *Loss-of-function mutations in a calcium-channel alpha1-subunit gene in Xp11.23 cause incomplete X-linked congenital stationary night blindness.* Nat Genet, 1998. **19**(3): p. 264-7.
142. Mori, Y., et al., *Primary structure and functional expression from complementary DNA of a brain calcium channel.* Nature, 1991. **350**(6317): p. 398-402.
143. Snutch, T.P., et al., *Rat brain expresses a heterogeneous family of calcium channels.* Proc Natl Acad Sci U S A, 1990. **87**(9): p. 3391-5.
144. Starr, T.V., W. Prystay, and T.P. Snutch, *Primary structure of a calcium channel that is highly expressed in the rat cerebellum.* Proc Natl Acad Sci U S A, 1991. **88**(13): p. 5621-5.
145. Cribbs, L.L., et al., *Cloning and characterization of alpha1H from human heart, a member of the T-type Ca2+ channel gene family.* Circ Res, 1998. **83**(1): p. 103-9.
146. Lee, J.H., et al., *Cloning and expression of a novel member of the low voltage-activated T-type calcium channel family.* J Neurosci, 1999. **19**(6): p. 1912-21.
147. Ertel, E.A., et al., *Nomenclature of voltage-gated calcium channels.* Neuron, 2000. **25**(3): p. 533-5.
148. Catterall, W.A., *Structure and function of voltage-gated ion channels.* Annu Rev Biochem, 1995. **64**: p. 493-531.
149. Coste de Bagneaux, P., et al., *Role of putative voltage-sensor countercharge D4 in regulating gating properties of CaV1.2 and CaV1.3 calcium channels.* Channels (Austin), 2018. **12**(1): p. 249-261.
150. Mangoni, M.E., et al., *Functional role of L-type CaV1.3 Ca2+ channels in cardiac pacemaker activity.* Proc Natl Acad Sci U S A, 2003. **100**(9): p. 5543-8.
151. Chen, X., et al., *Calcium influx through CaV1.2 is a proximal signal for pathological cardiomyocyte hypertrophy.* J Mol Cell Cardiol, 2011. **50**(3): p. 460-70.

152. Sinnegger-Brauns, M.J., et al., *Expression and 1,4-dihydropyridine-binding properties of brain L-type calcium channel isoforms.* Mol Pharmacol, 2009. **75**(2): p. 407-14.
153. Seisenberger, C., et al., *Functional embryonic cardiomyocytes after disruption of the L-type alpha1C (CaV1.2) calcium channel gene in the mouse.* J Biol Chem, 2000. **275**(50): p. 39193-9.
154. Rosati, B., et al., *Robust L-type calcium current expression following heterozygous knockout of the CaV1.2 gene in adult mouse heart.* J Physiol, 2011. **589**(Pt 13): p. 3275-88.
155. Splawski, I., et al., *Severe arrhythmia disorder caused by cardiac L-type calcium channel mutations.* Proc Natl Acad Sci U S A, 2005. **102**(23): p. 8089-96; discussion 8086-8.
156. Dick, I.E., et al., *Arrhythmogenesis in Timothy Syndrome is associated with defects in Ca(2+)-dependent inactivation.* Nat Commun, 2016. **7**: p. 10370.
157. Erxleben, C., et al., *Cyclosporin and Timothy syndrome increase mode 2 gating of CaV1.2 calcium channels through aberrant phosphorylation of S6 helices.* Proc Natl Acad Sci U S A, 2006. **103**(10): p. 3932-7.
158. Betzenhauser, M.J., G.S. Pitt, and C. Antzelevitch, *Calcium Channel Mutations in Cardiac Arrhythmia Syndromes.* Curr Mol Pharmacol, 2015. **8**(2): p. 133-42.
159. Santana, L.F., E.P. Cheng, and W.J. Lederer, *How does the shape of the cardiac action potential control calcium signaling and contraction in the heart?* J Mol Cell Cardiol, 2010. **49**(6): p. 901-3.
160. Grant, A.O., *Cardiac ion channels.* Circ Arrhythm Electrophysiol, 2009. **2**(2): p. 185-94.
161. Priest, B.T. and J.S. McDermott, *Cardiac ion channels.* Channels (Austin), 2015. **9**(6): p. 352-9.
162. Franzini-Armstrong, C., F. Protasi, and V. Ramesh, *Shape, size, and distribution of Ca(2+) release units and couplons in skeletal and cardiac muscles.* Biophys J, 1999. **77**(3): p. 1528-39.
163. Cannell, M.B., H. Cheng, and W.J. Lederer, *The control of calcium release in heart muscle.* Science, 1995. **268**(5213): p. 1045-9.
164. Inoue, M. and J.H. Bridge, *Ca2+ sparks in rabbit ventricular myocytes evoked by action potentials: involvement of clusters of L-type Ca2+ channels.* Circ Res, 2003. **92**(5): p. 532-8.
165. Santana, L.F., et al., *Relation between the sarcolemmal Ca2+ current and Ca2+ sparks and local control theories for cardiac excitation-contraction coupling.* Circ Res, 1996. **78**(1): p. 166-71.
166. Amin, A.S., H.L. Tan, and A.A. Wilde, *Cardiac ion channels in health and disease.* Heart Rhythm, 2010. **7**(1): p. 117-26.
167. Collier, M.L., et al., *Calcium-induced calcium release in smooth muscle: loose coupling between the action potential and calcium release.* J Gen Physiol, 2000. **115**(5): p. 653-62.
168. Saad, M., et al., *Ranolazine in Cardiac Arrhythmia.* Clin Cardiol, 2016. **39**(3): p. 170-8.
169. McDonagh, M.S., K.B. Eden, and K. Peterson, in *Drug Class Review: Calcium Channel Blockers: Final Report*. 2005: Portland (OR).
170. Fleckenstein, A., *History of calcium antagonists.* Circ Res, 1983. **52**(2 Pt 2): p. I3-16.

171. Lee, K.S. and R.W. Tsien, *Mechanism of calcium channel blockade by verapamil, D600, diltiazem and nitrendipine in single dialysed heart cells.* Nature, 1983. **302**(5911): p. 790-4.
172. McDonald, T.F., D. Pelzer, and W. Trautwein, *Cat ventricular muscle treated with D600: characteristics of calcium channel block and unblock.* J Physiol, 1984. **352**: p. 217-41.
173. Sanguinetti, M.C. and R.S. Kass, *Voltage-dependent block of calcium channel current in the calf cardiac Purkinje fiber by dihydropyridine calcium channel antagonists.* Circ Res, 1984. **55**(3): p. 336-48.
174. Striessnig, J., et al., *Structural basis of drug binding to L Ca2+ channels.* Trends Pharmacol Sci, 1998. **19**(3): p. 108-15.
175. Tikhonov, D.B. and B.S. Zhorov, *Structural model for dihydropyridine binding to L-type calcium channels.* J Biol Chem, 2009. **284**(28): p. 19006-17.
176. Tang, L., et al., *Structural basis for inhibition of a voltage-gated Ca(2+) channel by Ca(2+) antagonist drugs.* Nature, 2016. **537**(7618): p. 117-121.
177. Catterall, W.A. and J. Striessnig, *Receptor sites for Ca2+ channel antagonists.* Trends Pharmacol Sci, 1992. **13**(6): p. 256-62.
178. Kuniyasu, A., et al., *Photochemical identification of transmembrane segment IVS6 as the binding region of semotiadil, a new modulator for the L-type voltage-dependent Ca2+ channel.* J Biol Chem, 1998. **273**(8): p. 4635-41.
179. Regulla, S., et al., *Identification of the site of interaction of the dihydropyridine channel blockers nitrendipine and azidopine with the calcium-channel alpha 1 subunit.* EMBO J, 1991. **10**(1): p. 45-9.
180. Kalasz, H., et al., *Identification of 1,4-dihydropyridine binding domains within the primary structure of the alpha 1 subunit of the skeletal muscle L-type calcium channel.* FEBS Lett, 1993. **331**(1-2): p. 177-81.
181. Peterson, B.Z., et al., *Analysis of the dihydropyridine receptor site of L-type calcium channels by alanine-scanning mutagenesis.* J Biol Chem, 1997. **272**(30): p. 18752-8.
182. Beyl, S., et al., *Different pathways for activation and deactivation in CaV1.2: a minimal gating model.* J Gen Physiol, 2009. **134**(3): p. 231-41; S1-2.
183. Hodgkin, A.L. and A.F. Huxley, *A quantitative description of membrane current and its application to conduction and excitation in nerve.* J Physiol, 1952. **117**(4): p. 500-44.
184. Armstrong, C.M. and F. Bezanilla, *Currents related to movement of the gating particles of the sodium channels.* Nature, 1973. **242**(5398): p. 459-61.
185. Zagotta, W.N., et al., *Shaker potassium channel gating. II: Transitions in the activation pathway.* J Gen Physiol, 1994. **103**(2): p. 279-319.
186. Yamaguchi, H., et al., *Critical role of conserved proline residues in the transmembrane segment 4 voltage sensor function and in the gating of L-type calcium channels.* Proc Natl Acad Sci U S A, 1999. **96**(4): p. 1357-62.
187. Tuluc, P., et al., *Two distinct voltage-sensing domains control voltage sensitivity and kinetics of current activation in CaV1.1 calcium channels.* J Gen Physiol, 2016. **147**(6): p. 437-49.
188. Jurkovicova-Tarabova, B., et al., *Role of individual S4 segments in gating of CaV3.1 T-type calcium channel by voltage.* Channels (Austin), 2018. **12**(1): p. 378-387.
189. Karmazinova, M., et al., *Contrasting the roles of the I-II loop gating brake in CaV3.1 and CaV3.3 calcium channels.* Pflugers Arch, 2015. **467**(12): p. 2519-27.

190. Pantazis, A., et al., *Functional heterogeneity of the four voltage sensors of a human L-type calcium channel.* Proc Natl Acad Sci U S A, 2014. **111**(51): p. 18381-6.
191. Limpitikul, W.B., et al., *A Precision Medicine Approach to the Rescue of Function on Malignant Calmodulinopathic Long-QT Syndrome.* Circ Res, 2017. **120**(1): p. 39-48.
192. Singh, A., et al., *C-terminal modulator controls Ca2+-dependent gating of Ca(v)1.4 L-type Ca2+ channels.* Nat Neurosci, 2006. **9**(9): p. 1108-16.
193. Alseikhan, B.A., et al., *Engineered calmodulins reveal the unexpected eminence of Ca2+ channel inactivation in controlling heart excitation.* Proc Natl Acad Sci U S A, 2002. **99**(26): p. 17185-90.
194. Bahring, R. and M. Covarrubias, *Mechanisms of closed-state inactivation in voltage-gated ion channels.* J Physiol, 2011. **589**(Pt 3): p. 461-79.
195. Lacinova, L., *Voltage-dependent calcium channels.* General Physiology and Biophysics, 2005. **24**: p. 3-78.
196. Fallon, J.L., et al., *Crystal structure of dimeric cardiac L-type calcium channel regulatory domains bridged by Ca2+* calmodulins.* Proc Natl Acad Sci U S A, 2009. **106**(13): p. 5135-40.
197. Neely, A., et al., *Ca(2+)-dependent inactivation of a cloned cardiac Ca2+ channel alpha 1 subunit (alpha 1C) expressed in Xenopus oocytes.* Biophys J, 1994. **66**(6): p. 1895-903.
198. Demers-Giroux, P.O., et al., *Cooperative activation of the T-type CaV3.2 channel: interaction between Domains II and III.* J Biol Chem, 2013. **288**(41): p. 29281-93.
199. Yan, Z., et al., *Structure of the Nav1.4-beta1 Complex from Electric Eel.* Cell, 2017. **170**(3): p. 470-482 e11.
200. Hering, S., et al., *Molecular determinants of inactivation in voltage-gated Ca2+ channels.* J Physiol, 2000. **528 Pt 2**: p. 237-49.
201. Isom, L.L., K.S. De Jongh, and W.A. Catterall, *Auxiliary subunits of voltage-gated ion channels.* Neuron, 1994. **12**(6): p. 1183-94.
202. Qin, N., et al., *Unique regulatory properties of the type 2a Ca2+ channel beta subunit caused by palmitoylation.* Proc Natl Acad Sci U S A, 1998. **95**(8): p. 4690-5.
203. Sokolov, S., et al., *Modulation of slow inactivation in class A Ca2+ channels by beta-subunits.* J Physiol, 2000. **527 Pt 3**: p. 445-54.
204. Olcese, R., et al., *The amino terminus of a calcium channel beta subunit sets rates of channel inactivation independently of the subunit's effect on activation.* Neuron, 1994. **13**(6): p. 1433-8.
205. Bean, B.P., *Nitrendipine block of cardiac calcium channels: high-affinity binding to the inactivated state.* Proc Natl Acad Sci U S A, 1984. **81**(20): p. 6388-92.
206. Wu, J., N. Yan, and Z. Yan, *Structure-Function Relationship of the Voltage-Gated Calcium Channel CaV1.1 Complex.* Adv Exp Med Biol, 2017. **981**: p. 23-39.
207. Armstrong, C.M. and F. Bezanilla, *Inactivation of the sodium channel. II. Gating current experiments.* J Gen Physiol, 1977. **70**(5): p. 567-90.
208. Hoshi, T., W.N. Zagotta, and R.W. Aldrich, *Biophysical and molecular mechanisms of Shaker potassium channel inactivation.* Science, 1990. **250**(4980): p. 533-8.

209. Zagotta, W.N., T. Hoshi, and R.W. Aldrich, *Restoration of inactivation in mutants of Shaker potassium channels by a peptide derived from ShB.* Science, 1990. **250**(4980): p. 568-71.
210. Stotz, S.C., et al., *Fast inactivation of voltage-dependent calcium channels. A hinged-lid mechanism?* J Biol Chem, 2000. **275**(32): p. 24575-82.
211. Marksteiner, R., et al., *Inactivation determinants in segment IIIS6 of Ca(v)3.1.* J Physiol, 2001. **537**(Pt 1): p. 27-34.
212. Berjukow, S., et al., *Amino acids in segment IVS6 and beta-subunit interaction support distinct conformational changes during Ca(v)2.1 inactivation.* J Biol Chem, 2001. **276**(20): p. 17076-82.
213. Stotz, S.C. and G.W. Zamponi, *Identification of inactivation determinants in the domain IIS6 region of high voltage-activated calcium channels.* J Biol Chem, 2001. **276**(35): p. 33001-10.
214. Abderemane-Ali, F., et al., *A Selectivity Filter Gate Controls Voltage-Gated Calcium Channel Calcium-Dependent Inactivation.* Neuron, 2019.
215. Soldatov, N.M., et al., *Molecular determinants of L-type Ca2+ channel inactivation. Segment exchange analysis of the carboxyl-terminal cytoplasmic motif encoded by exons 40-42 of the human alpha1C subunit gene.* J Biol Chem, 1998. **273**(2): p. 957-63.
216. Hering, S., et al., *Transfer of high sensitivity for benzothiazepines from L-type to class A (BI) calcium channels.* J Biol Chem, 1996. **271**(40): p. 24471-5.
217. Herlitze, S., et al., *Molecular determinants of inactivation and G protein modulation in the intracellular loop connecting domains I and II of the calcium channel alpha1A subunit.* Proc Natl Acad Sci U S A, 1997. **94**(4): p. 1512-6.
218. Bourinet, E., et al., *Splicing of alpha 1A subunit gene generates phenotypic variants of P- and Q-type calcium channels.* Nat Neurosci, 1999. **2**(5): p. 407-15.
219. Spaetgens, R.L. and G.W. Zamponi, *Multiple structural domains contribute to voltage-dependent inactivation of rat brain alpha(1E) calcium channels.* J Biol Chem, 1999. **274**(32): p. 22428-36.
220. Beyl, S., et al., *Neutralisation of a single voltage sensor affects gating determinants in all four pore-forming S6 segments of Ca(V)1.2: a cooperative gating model.* Pflugers Arch, 2012. **464**(4): p. 391-401.
221. Sokolov, S., E. Timin, and S. Hering, *On the role of Ca(2+)- and voltage-dependent inactivation in Ca(v)1.2 sensitivity for the phenylalkylamine (-)gallopamil.* Circ Res, 2001. **89**(8): p. 700-8.
222. Zhang, X., et al., *Crystal structure of an orthologue of the NaChBac voltage-gated sodium channel.* Nature, 2012. **486**(7401): p. 130-4.
223. Bezanilla, F. and C.A. Villalba-Galea, *The gating charge should not be estimated by fitting a two-state model to a Q-V curve.* J Gen Physiol, 2013. **142**(6): p. 575-8.
224. !!! INVALID CITATION !!!
225. Stotz, S.C., S.E. Jarvis, and G.W. Zamponi, *Functional roles of cytoplasmic loops and pore lining transmembrane helices in the voltage-dependent inactivation of HVA calcium channels.* J Physiol, 2004. **554**(Pt 2): p. 263-73.
226. Bao, H., et al., *Voltage-insensitive gating after charge-neutralizing mutations in the S4 segment of Shaker channels.* J Gen Physiol, 1999. **113**(1): p. 139-51.
227. Capes, D.L., et al., *Domain IV voltage-sensor movement is both sufficient and rate limiting for fast inactivation in sodium channels.* J Gen Physiol, 2013. **142**(2): p. 101-12.

228. Miceli, F., et al., *Gating consequences of charge neutralization of arginine residues in the S4 segment of K(v)7.2, an epilepsy-linked K+ channel subunit.* Biophys J, 2008. **95**(5): p. 2254-64.
229. Cuello, L.G., et al., *Structural mechanism of C-type inactivation in K(+) channels.* Nature, 2010. **466**(7303): p. 203-8.
230. Choi, K.L., R.W. Aldrich, and G. Yellen, *Tetraethylammonium blockade distinguishes two inactivation mechanisms in voltage-activated K+ channels.* Proc Natl Acad Sci U S A, 1991. **88**(12): p. 5092-5.
231. Cuello, L.G., et al., *Structural basis for the coupling between activation and inactivation gates in K(+) channels.* Nature, 2010. **466**(7303): p. 272-5.
232. Kiss, L., J. LoTurco, and S.J. Korn, *Contribution of the selectivity filter to inactivation in potassium channels.* Biophys J, 1999. **76**(1 Pt 1): p. 253-63.
233. Rios, E., D. Gillespie, and C. Franzini-Armstrong, *The binding interactions that maintain excitation-contraction coupling junctions in skeletal muscle.* J Gen Physiol, 2019.
234. Pinggera, A. and J. Striessnig, *CaV 1.3 (CACNA1D) L-type Ca(2+) channel dysfunction in CNS disorders.* J Physiol, 2016. **594**(20): p. 5839-5849.
235. Snutch T.P., Peloquin J., Mathews E., and McRory J.E. Molecular Properties of Voltage-Gated Calcium Channels. Madame Curie Bioscience Database, 2013
236. W. Forth, D. Henschler, W. Rummel, Pharmakologie and Toxikologie, 11. Auflage 2013
237. Zahradnik, I., I. Minarovic, and A. Zahradnikova, *Inhibition of the cardiac L-type calcium channel current by antidepressant drugs.* J Pharmacol Exp Ther, 2008. **324**(3): p. 977-84.
238. Van Petegem, F., F.C. Chatelain, and D.L. Minor, Jr., *Insights into voltage-gated calcium channel regulation from the structure of the CaV1.2 IQ domain-Ca2+/calmodulin complex.* Nat Struct Mol Biol, 2005. **12**(12): p. 1108-15.
239. Ben-Johny, M., et al., *Towards a Unified Theory of Calmodulin Regulation (Calmodulation) of Voltage-Gated Calcium and Sodium Channels.* Curr Mol Pharmacol, 2015. **8**(2): p. 188-205.
240. Hodgkin AL, Huxley AF. Currents carried by sodium and potassium ions through the membrane of the giant axon of Loligo. J Physiol. 1952a;116:449–472.
241. Xie, C., X.G. Zhen, and J. Yang, *Localization of the activation gate of a voltage-gated Ca2+ channel.* J Gen Physiol, 2005. **126**(3): p. 205-12.

Ich habe mich bemüht, sämtliche Inhaber der Bildrechte ausfindig zu machen und ihre Zustimmung zur Verwendung der Bilder in dieser Arbeit eingeholt. Sollte dennoch eine Urheberrechtsverletzung bekannt werden, ersuche ich um Meldung bei mir.